bioRxiv preprint doi: https://doi.org/10.1101/2021.10.19.465059; this version posted October 20, 2021. The copyright holder for this preprint (which was not certified by peer review) is the author/funder, who has granted bioRxiv a license to display the preprint in perpetuity. It is made available under aCC-BY-NC-ND 4.0 International license.

Identification of novel therapeutic targets for polyglutamine toxicity disorders that target mitochondrial fragmentation

Annika Traa[1,2]*, Emily Machiela[3*], Paige D. Rudich[1,2], Sonja K. Soo[1,2], Megan M. Senchuk[3], Jeremy M. Van Raamsdonk[1,2,3,4,5]

[1]Department of Neurology and Neurosurgery, McGill University, Montreal, Quebec, H4A 3J1, Canada
[2]Metabolic Disorders and Complications Program, and Brain Repair and Integrative Neuroscience Program, Research Institute of the McGill University Health Centre, Montreal, Quebec, H4A 3J1, Canada
[3]Laboratory of Aging and Neurodegenerative Disease, Center for Neurodegenerative Science, Van Andel Research Institute, Grand Rapids MI 49503, USA
[4]Division of Experimental Medicine, Department of Medicine, McGill University, Montreal, Quebec, Canada
[5]Department of Genetics, Harvard Medical School, Boston MA 02115, USA

*these authors contributed equally to this work

Short title: Mitochondrial dynamics and polyglutamine toxicity

Corresponding author:
Jeremy M. Van Raamsdonk
Department of Neurology and Neurosurgery, McGill University
MeDiC and BRaIN Programs, McGill University Health Centre
1001 Decarie Boulevard, Montreal, Quebec, H4A 3J1
514-934-1934 ext. 76157
jeremy.vanraamsdonk@mcgill.ca
ORCID iD: 0000-0001-8376-9605

bioRxiv preprint doi: https://doi.org/10.1101/2021.10.19.465059; this version posted October 20, 2021. The copyright holder for this preprint (which was not certified by peer review) is the author/funder, who has granted bioRxiv a license to display the preprint in perpetuity. It is made available under aCC-BY-NC-ND 4.0 International license.

Abstract

Huntington's disease (HD) is one of at least nine polyglutamine toxicity disorders caused by a trinucleotide CAG repeat expansion, all of which lead to age-onset neurodegeneration. Mitochondrial dynamics and function are disrupted in HD and other polyglutamine toxicity disorders. While multiple studies have found beneficial effects from decreasing mitochondrial fragmentation in HD models by disrupting the mitochondrial fission protein DRP1, disrupting DRP1 can also have detrimental consequences in wild-type animals and HD models. In this work, we examine the effect of decreasing mitochondrial fragmentation in a neuronal *C. elegans* model of polyglutamine toxicity called Neur-67Q. We find that Neur-67Q worms have deficits in mitochondrial morphology in GABAergic neurons and decreased mitochondrial function. Disruption of *drp-1* eliminates differences in mitochondrial morphology and rescues deficits in both movement and longevity in Neur-67Q worms. In testing twenty-four RNA interference (RNAi) clones that decrease mitochondrial fragmentation, we identified eleven clones that increase movement and extend lifespan in Neur-67Q worms. Overall, we show that decreasing mitochondrial fragmentation may be an effective approach to treat polyglutamine toxicity disorders and identify multiple novel genetic targets that circumvent the potential negative side effects of disrupting the primary mitochondrial fission gene *drp-1.*

Keywords: *C. elegans*; Huntington's disease; mitochondria; mitochondrial dynamics; polyglutamine toxicity disorder

bioRxiv preprint doi: https://doi.org/10.1101/2021.10.19.465059; this version posted October 20, 2021. The copyright holder for this preprint (which was not certified by peer review) is the author/funder, who has granted bioRxiv a license to display the preprint in perpetuity. It is made available under aCC-BY-NC-ND 4.0 International license.

Significance Statement

Polyglutamine toxicity disorders are caused by a trinucleotide CAG repeat expansion that leads to neurodegeneration. Both mitochondrial dynamics and function are disrupted in these disorders. In this work we use a simple genetic model organism, the worm *C. elegans,* to define the role of mitochondrial morphology in polyglutamine toxicity disorders. We show that CAG repeat expansion is sufficient to disrupt mitochondrial morphology and that genetic strategies that decrease mitochondrial fragmentation are beneficial in a neuronal model of polyglutamine toxicity. This work identifies multiple novel genes that are protective in worm models of polyglutamine toxicity, which may serve as potential therapeutic targets for Huntington's disease and other polyglutamine toxicity disorders.

bioRxiv preprint doi: https://doi.org/10.1101/2021.10.19.465059; this version posted October 20, 2021. The copyright holder for this preprint (which was not certified by peer review) is the author/funder, who has granted bioRxiv a license to display the preprint in perpetuity. It is made available under aCC-BY-NC-ND 4.0 International license.

Introduction

Huntington's disease (HD) is an adult-onset neurodegenerative disease caused by a trinucleotide CAG repeat expansion in the first exon of the *HTT* gene. The resulting expansion of the polyglutamine tract in the huntingtin protein causes a toxic gain of function that contributes to disease pathogenesis. HD is the most common of at least nine polyglutamine toxicity disorders including spinal and bulbar muscular atrophy (SBMA), dentatorubral-pallidoluysian atrophy (DRPLA), and spinocerebellar ataxia types 1, 2, 3, 6, 7 and 17 (SCA1, SCA2, SCA3, SCA6, SCA7, SCA17) [1,2]. Each disease occurs due to an expansion of a CAG repeat above a specific threshold number of repeats. The minimum number of disease-causing CAG repeats range from 21 CAG repeats (SCA6) to 55 CAG repeats (SCA3). These disorders are all unique neurodegenerative diseases that typically present in mid-life, but can present earlier in life with larger CAG repeat expansions [3,4]. The genes responsible for these disorders appear to be unrelated except for the presence of the CAG repeat sequence, indicating that CAG repeat expansion, independent of the genetic context, is likely sufficient to cause disease.

Multiple lines of evidence suggest a role for mitochondrial dysfunction in the pathogenesis of polyglutamine toxicity disorders [5,6]. Both HD patients and animal models of the disease display several signs of mitochondrial dysfunction including decreased activity in the complexes of the mitochondrial electron transport chain [7], increased lactate production in the brain [8], decreased levels of ATP production [9], lowered mitochondrial membrane potentials [10], and impaired mitochondrial trafficking [11]. While less well studied than HD, other polyglutamine toxicity disorders also have evidence of mitochondrial deficits [12-15].

Mitochondrial fragmentation is a consistent feature of HD as it occurs in HD cell lines, HD worm models, HD mouse models and cells derived from HD patients [16-23]. Mitochondrial fragmentation has also been observed in models of other polyglutamine toxicity disorders, including SCA3, SCA7, and SBMA [24-26]. This suggests that CAG repeat expansion may be sufficient to cause mitochondrial fragmentation.

bioRxiv preprint doi: https://doi.org/10.1101/2021.10.19.465059; this version posted October 20, 2021. The copyright holder for this preprint (which was not certified by peer review) is the author/funder, who has granted bioRxiv a license to display the preprint in perpetuity. It is made available under aCC-BY-NC-ND 4.0 International license.

In order to decrease HD-associated mitochondrial fragmentation, multiple groups have targeted the mitochondrial fission protein DRP1 in models of HD. While disruption of DRP1 typically has beneficial effects in HD models [16,17,19], it has also been found to exacerbate disease phenotypes [23]. The difference in effect may be due to the level of DRP1 disruption, as deletion of *drp-1* was detrimental in an HD model while RNAi knockdown of *drp-1* in the same model had mixed effects [23]. Decreasing DRP1 levels can also be detrimental in a wild-type background [23,27-32]. Thus, reducing mitochondrial fragmentation through other genetic targets may be a more ideal therapeutic strategy for HD and other polyglutamine toxicity disorders than disrupting DRP1.

In this work, we show that CAG repeat expansion is sufficient to disrupt mitochondrial morphology and function in a neuronal model of polyglutamine toxicity. The neuronal model of polyglutamine toxicity also displays deficits in movement and lifespan, which are ameliorated by deletion of *drp-1*. Using this model, we performed a targeted RNAi screen and identified eleven novel genetic targets that improve movement and increase lifespan. Overall, this work demonstrates that decreasing mitochondrial fragmentation may be an effective therapeutic strategy for polyglutamine toxicity disorders and identifies multiple potential genetic therapeutic targets for these disorders.

bioRxiv preprint doi: https://doi.org/10.1101/2021.10.19.465059; this version posted October 20, 2021. The copyright holder for this preprint (which was not certified by peer review) is the author/funder, who has granted bioRxiv a license to display the preprint in perpetuity. It is made available under aCC-BY-NC-ND 4.0 International license.

Materials and Methods

Strains

N2 (WT)

AM102 *rmIs111[rgef-1p::40Q:YFP]* referred to as Neur-40Q

AM717 *rmIs284[rgef-1p::67Q:YFP]* referred to as Neur-67Q

JVR258 *drp-1*(*tm1108*);*rmIs284[rgef-1p::67Q:YFP]*

JVR438 *rmIs284[rgef-1p::67Q:YFP]; sid-1(pk3321); uIs69 [pCFJ90 (myo-2p::mCherry) + unc-119p::sid-1]*

JVR443 *rmIs284[rgef-1p::67Q:YFP]; uIs69 [pCFJ90 (myo-2p::mCherry) + unc-119p::sid-1]*

PHX3820 *sybIs3820[rab-3p::tomm-20::mScarlet]* referred to as mito-mScarlet

JVR611 *rmIs284[rgef-1p::67Q:YFP];drp-1(tm1108); sybIs3820[rab-3p::tomm-20::mScarlet]* referred to as Neur-67Q;*drp-1;*mito-mScarlet

JVR612 *rmIs284[rgef-1p::67Q:YFP]; sybIs3820[rab-3p::tomm-20::mScarlet]* referred to as Neur-67Q;mito-mScarlet

JVR613 *drp-1(tm1108); sybIs3820[rab-3p::tomm-20::mScarlet]* referred to as *drp-1;*mito-mScarlet

MQ1753 *drp-1* (*tm1108*)

TU3401 *sid-1(pk3321); uIs69 [pCFJ90 (myo-2p::mCherry) + unc-119p::sid-1]*

Strains were maintained at 20°C on NGM plates seeded with OP50 bacteria. The Neur-67Q model of HD is an integrated line that has been well characterized previously [33]. All crosses were confirmed by genotyping using PCR for deletion mutations, sequencing for point mutations and confirmation of fluorescence for fluorescent transgenes.

Generation of strains to monitor mitochondrial morphology in GABA neurons

The *rab-3p::tomm-20::mScarlet* strain was generated by SunyBiotech Co. Ltd. The 1208 bp *rab-3* promoter sequence (Addgene Plasmid #110880) was inserted directly upstream of the N-terminal TOMM-20 coding region. The first 47 amino acids of TOMM-20 were connected through a flexible linker (3xGGGGS) to the N-terminal of wrmScarlet [34]. The strain was

bioRxiv preprint doi: https://doi.org/10.1101/2021.10.19.465059; this version posted October 20, 2021. The copyright holder for this preprint (which was not certified by peer review) is the author/funder, who has granted bioRxiv a license to display the preprint in perpetuity. It is made available under aCC-BY-NC-ND 4.0 International license.

generated through microinjection of *rab-3p::tomm-20::mScarlet* in the pS1190 plasmid (20 ng/µl) into wild-type N2 worms. The transgenic strain was integrated by γ-irradiation and the outcrossed 5X to remove background mutations.

Confocal imaging and quantification

Mitochondrial morphology was imaged and quantified using worms that express mitochondrially-targeted mScarlet specifically in neurons (*rab-3p::tomm-20::mScarlet*). Worms at day 1 or day 7 of adulthood were mounted on 2% agar pads and immobilized using 10 µM levamisole. Worms were imaged under a 63x objective lens on a Zeiss LSM 780 confocal microscope. All conditions were kept the same for all images. Single plane images were collected for a total of 25 young adult worms over 3 biological replicates for each strain. Quantification of mitochondrial morphology was performed using ImageJ. Segmentation analysis was done using the SQUASSH (segmentation and quantification of subcellular shapes) plugin. Particle analysis was then used to quantify number of mitochondria, mitochondrial area, axonal mitochondrial load, mitochondrial circularity and maximum Feret's diameter (an indicator of particle length). Axonal load was calculated as the total mitochondrial area (μm^2) in a region of interest (ROI), per length (µm) of axon in the ROI. For representative images, mScarlet and YFP channels were merged. We observed some bleed-through of YFP into the red channel for strains expressing the 67Q-YFP transgene. Particles that showed up in the mScarlet images as a result of YFP bleed-through were manually excluded from morphology quantification based on the numbered particle mask output from the ImageJ particle analyzer.

Oxygen consumption

To measure basal oxygen consumption, a Seahorse XF_e96 analyzer (Seahorse bioscience Inc., North Billerica, MA, USA)[35] was used. Adult day 1 worms were washed in M9 buffer (22 mM KH_2PO_4, 34 mM NA_2HPO_4, 86 mM NaCl, 1 mM $MgSO_4$) and pipetted in calibrant (~50 worms per well) into a Seahorse 96-well plate. Oxygen consumption rate was measured six times. One day before the assay, well probes were hydrated in 175 µL of Seahorse calibrant solution overnight. The heating incubator was turned off to allow the Seahorse machine to reach room

bioRxiv preprint doi: https://doi.org/10.1101/2021.10.19.465059; this version posted October 20, 2021. The copyright holder for this preprint (which was not certified by peer review) is the author/funder, who has granted bioRxiv a license to display the preprint in perpetuity. It is made available under aCC-BY-NC-ND 4.0 International license.

temperature before placing worms inside. Rates of respiration were normalized to the number of worms per well. Plate readings were within 20 minutes of introducing the worms into the well and normalized relative to the number of worms per well.

ATP production

To measure ATP production, a luminescence-based ATP kit was used [36]. Approximately 200 age-synchronized worms were collected in deionized water before being washed and freeze-thawed three times. A Bioruptor (Diagenode) was used to sonicate the worm pellet for 30 cycles of alternating 30 seconds on and 30 seconds off. The pellet was boiled for 15 minutes to release ATP. The pellet was then centrifuged at 11,000 $\times$ *g* for 10 minutes at 4°C and the resulting supernatant was collected. A Molecular Probes ATP determination Kit (Life Technologies) was used to measure ATP. Luminescence was normalized to protein levels determined by a Pierce BCA protein determination kit (Thermo Scientific).

Rate of movement

To measure rate of movement, thrashing rate in liquid was assessed using video-tracking and computer analysis [37]. Approximately 50 day 1 adult worms were placed in M9 buffer on an unseeded NGM plate. An Allied Vision Tech Stingray F-145 B Firewire Camera (Allied Vision, Exton, PA, USA) was used to capture videos at 1024×768 resolution and 8-bit using the MATLAB image acquisition toolbox. The wrMTrck plugin for ImageJ (http://www.phage.dk/plugins) was used to analyze rate of movement.

Lifespan

To measure lifespan, worms were placed on nematode growth media (NGM) agar plates containing 25 µM 5-fluoro-2'-deoxyuridine (FUdR). FUdR was used to reduce the progeny development. At 25 µM concentration of FUdR, progeny development into adulthood is not completely prevented in the first generation so animals were transferred to fresh plates after 4 days [38]. Worms were moved to fresh plates weekly and survival was observed by gentle

bioRxiv preprint doi: https://doi.org/10.1101/2021.10.19.465059; this version posted October 20, 2021. The copyright holder for this preprint (which was not certified by peer review) is the author/funder, who has granted bioRxiv a license to display the preprint in perpetuity. It is made available under aCC-BY-NC-ND 4.0 International license.

prodding every 2 days. Lifespan experiments were conducted with three replicates of 30 worms each.

Brood size

To determine brood size, individual young adult worms were placed onto agar plates and transferred every day to new plates until progeny production stopped. Plates of resulting progeny were quantified when adulthood was reached. Experiments were conducted with three replicates of 5 worms each.

Post-embryonic development

To measure post-embryonic development (PED), eggs were moved to agar plates and left to hatch for 3 hours. L1 worms that were newly hatched were transferred to a new plate. The PED time was considered the total time from hatching to the young adult stage. Experiments were conducted with three replicates of 20 animals each.

Quantitative reverse-transcription PCR (qPCR)

To quantify mRNA levels, pre-fertile young adult worms were harvested in Trizol as previously described [39]. Three biological replicates for N2, BW-40Q, and BW-Htt74Q worms were collected to quantify gene expression. A High-Capacity cDNA Reverse Transcription kit (Life Technologies/Invitrogen) was used to convert mRNA to cDNA. A FastStart Universal SYBR Green kit (Roche) in an AP Biosystems real-time PCR machine were used to perform qPCR [40,41]. Primer sequences used:

yfp (L-GACGACGGCAACTACAAGAC, R-TCCTTGAAGTCGATGCCCTT).

RNAi

To knockdown gene expression, sequence-verified RNAi clones were grown approximately 12 hours in LB with 50 µg/ml carbenicillin. Bacteria cultures were 5x concentrated and seeded onto NGM plates containing 5 mM IPTG and 50 µg/ml carbenicillin. Plates were incubated at room temperature for 2 days to induce RNAi. For the L4 parental paradigm, in which RNAi

bioRxiv preprint doi: https://doi.org/10.1101/2021.10.19.465059; this version posted October 20, 2021. The copyright holder for this preprint (which was not certified by peer review) is the author/funder, who has granted bioRxiv a license to display the preprint in perpetuity. It is made available under aCC-BY-NC-ND 4.0 International license.

knockdown began in the parental generation, L4 worms were plated on RNAi plates for one day and then transferred to a new plate as gravid adults. After 24 hours, the worms were removed from the plates. The resulting progeny from these worms were analyzed. RNAi experiments were conducted at 20°C.

Experimental Design and Statistical Analysis

All experiments were performed with experimenters blinded to the genotype of the worms. Worms used for experiments were randomly selected from maintenance plates. A minimum of three biological replicates, in which independent population of worms tested on different days, were performed for each experiment. Automated computer analysis was performed in assays where possible to eliminate potential bias. Power calculations were not used to determine sample size for experiments since sample size used in *C. elegans* studies are typically larger than required for observing a difference that is statistically significant. Three biological replicates were used for measurements of mitochondrial morphology. At least six replicates of ~50 worms each were used for measurements of oxygen consumption. Three biological replicates of ~200 worms each were used for ATP measurements. Three biological replicates of 60 mm plate of worms were used for mRNA measurements. At least three biological replicates of ~40 worms each were used for the thrashing assays. Three biological replicates of 30 worms each were used for lifespan assays. Six individual worms were used for measuring brood size. Three biological replicates of 25 worms each were used to measure post-embryonic development time. GraphPad Prism was used to perform statistical analysis. One-way, two-way or repeated measures ANOVA were used to determine statistically significant differences between groups with Dunnett's or Bonferroni's multiple comparisons test. For analysis of lifespan, Kaplan-Meier survival plot were graphed and the Log-rank test was used to determine significant differences between two groups. This study has no pre-specified primary endpoint. Sample size calculations were not performed.

bioRxiv preprint doi: https://doi.org/10.1101/2021.10.19.465059; this version posted October 20, 2021. The copyright holder for this preprint (which was not certified by peer review) is the author/funder, who has granted bioRxiv a license to display the preprint in perpetuity. It is made available under aCC-BY-NC-ND 4.0 International license.

Results

Mitochondrial morphology and function are disrupted in a neuronal model of polyglutamine toxicity

In order to study the effect of polyglutamine toxicity on mitochondrial dynamics in neurons, we utilized a well-characterized model that expresses a polyglutamine protein containing 67 glutamines tagged with YFP under the pan-neuronal *rgef-1* promoter [33]. These worms will be referred to as Neur-67Q worms. To visualize mitochondrial morphology in GABAergic neurons, we generated a new strain expressing mScarlet fused with the N-terminus of TOMM-20 (translocase of outer mitochondrial membrane 20), thus targeting the red fluorescent protein mScarlet to the mitochondria. These worms (*rab-3p::tomm-20::mScarlet*) will be referred to as mito-mScarlet worms. After crossing Neur-67Q worms to mito-mScarlet worms, we examined mitochondrial morphology in the dorsal nerve cord.

We found that Neur-67Q worms exhibit mitochondrial fragmentation (**Fig. S1A**). Compared to mito-mScarlet control worms, Neur-67Q; mito-mScarlet worms have a decreased number of mitochondria (**Fig. S1B**). Although mitochondrial area was not significantly affected by CAG repeat expansion (**Fig. S1C**), Neur-67Q worms exhibit a decreased axonal mitochondrial load (**Fig. S1D**), which is calculated as mitochondria area per length of axon. In addition, the shape of the mitochondria is affected as Neur-67Q;mito-mScarlet worms have more circular mitochondria (**Fig. S1E**) and a decreased maximum Feret's diameter of the mitochondria (**Fig. 1E**), which is the maximum distance between two parallel tangents to the mitochondria.

To determine if the differences in mitochondrial morphology affect mitochondrial function, we measured the rate of oxidative phosphorylation (oxygen consumption) and energy production (ATP levels). We found that Neur-67Q worms have increased oxygen consumption (**Fig. S2A**) but decreased levels of ATP (**Fig. S2B**). This suggests that the mitochondria in Neur-67Q are less efficient than in wild-type worms, possibly due to mitochondrial uncoupling. Combined, these

bioRxiv preprint doi: https://doi.org/10.1101/2021.10.19.465059; this version posted October 20, 2021. The copyright holder for this preprint (which was not certified by peer review) is the author/funder, who has granted bioRxiv a license to display the preprint in perpetuity. It is made available under aCC-BY-NC-ND 4.0 International license.

results show the presence of a disease-length CAG repeat expansion is sufficient to disrupt mitochondrial morphology and function.

Differences in mitochondrial morphology in neuronal model of polyglutamine toxicity are exacerbated with increasing age

To determine the effect of age on mitochondrial dynamics in Neur-67Q worms, we imaged and quantified mitochondrial morphology in worms at day 7 of adulthood. As in young adult worms, adult day 7 Neur-67Q worms exhibit mitochondrial fragmentation and a decrease in axonal mitochondria, which is much greater than observed in day 1 adult worms (**Fig. 1A**). Quantification of mitochondrial morphology revealed that day 7 Neur-67Q worms have decreased mitochondrial number (**Fig. 1B**), decreased mitochondrial area (**Fig. 1C**), decreased axonal mitochondrial load (**Fig. 1D**), increased mitochondrial circularity (**Fig. 1E**) and decreased Feret's diameter of the mitochondria (**Fig. 1F**). These results indicate that aged Neur-67Q worms have a highly disconnected mitochondrial network morphology. Furthermore, the percentage decreases in mitochondrial number (-27% day 1 versus -64% day 7), mitochondrial area (-10% day 1 versus -22% day 7) and axonal mitochondrial load (-35% day 1 versus -70% day 7) were all much greater at day 7 than at day 1 indicating that the deficits in mitochondrial morphology in Neur-67Q worms worsen with age (**Fig. S3**).

Disruption of mitochondrial fission is beneficial in a neuronal model of polyglutamine toxicity

As disruption of *drp-1* has been shown to ameliorate phenotypic deficits in various models of HD, we examined whether disruption of *drp-1* would be beneficial in Neur-67Q worms. We found that deletion of *drp-1* significantly improved mobility (**Fig. 2A**) and increased lifespan (**Fig. 2B**) in Neur-67Q worms. While the *drp-1* deletion decreased fertility (**Fig. 2C**) and slowed development (**Fig. 2D**) in wild-type worms, it did not affect either of these phenotypes in Neur-67Q worms. Finally, we examined the effect of *drp-1* deletion on mitochondrial function in Neur-67Q worms. We found that the increased oxygen consumption observed in Neur-67Q worms is significantly decreased by disruption of *drp-1* (**Fig. 2E**). However, the *drp-1* deletion was unable to increase the low ATP levels in Neur-67Q worms, and decreased ATP levels in

bioRxiv preprint doi: https://doi.org/10.1101/2021.10.19.465059; this version posted October 20, 2021. The copyright holder for this preprint (which was not certified by peer review) is the author/funder, who has granted bioRxiv a license to display the preprint in perpetuity. It is made available under aCC-BY-NC-ND 4.0 International license.

wild-type worms (**Fig. 2F**). Although the effects of *drp-1* deletion in Neur-67Q worms are primarily beneficial, the loss of *drp-1* increased expression of the disease-length polyglutamine mRNA (**Fig. S4**), as we and others have previously observed [16,23]. Since increased levels of polyglutamine protein would cause more toxicity, the protective effects of *drp-1* deletion may be greater if polyglutamine mRNA levels were unaffected.

To ensure that the beneficial effects of the *drp-1* deletion in Neur-67Q worms are caused by the disruption of *drp-1,* we examined the effect of *drp-1* RNAi in Neur-67Q worms. Because most *C. elegans* neurons are resistant to RNAi knockdown [42], we first crossed Neur-67Q worms to a worm strain that exhibits enhanced RNAi knockdown specifically in the neurons but is resistant to RNAi in other tissues [43]. In the resulting strain (Neur-67Q;*sid-1;unc-119p::sid-1*), RNAi is only active in the nervous system.

As with the *drp-1* deletion, knocking down *drp-1* expression throughout life increased the rate of movement (**Fig. S5A**) and increased lifespan (**Fig. S5B**) in Neur-67Q worms, while having no effect on fertility in Neur-67Q worms (**Fig. S5C**). As with the *drp-1* deletion, *drp-1* RNAi decreased both oxygen consumption and ATP levels in Neur-67Q worms (**Fig. S5D,E**).

Disruption of mitochondrial fission decreases mitochondrial fragmentation in neurons

Having shown that *drp-1* deletion ameliorates phenotypic deficits in Neur-67Q worms, we wondered whether the alterations in mitochondrial morphology were also corrected. Accordingly, we imaged and quantified mitochondrial morphology in Neur-67Q;*drp-1* worms at day 1 (**Fig. S6**) and day 7 (**Fig. 3**) of adulthood. At day 1 of adulthood, disruption of *drp-1* markedly elongated the neuronal mitochondria leading to decreased mitochondrial fragmentation in both Neur-67Q worms and wild-type worms (**Fig. S6A**). Quantification of these differences revealed that deletion of *drp-1* results in significantly decreased numbers of mitochondria (**Fig. S6B**), significantly increased mitochondrial area (**Fig. S6C**), significantly increased axonal mitochondrial load (**Fig. S6D**), significantly decreased mitochondrial circularity (**Fig. S6E**) and significantly increased Feret's diameter (**Fig. S6F**).

bioRxiv preprint doi: https://doi.org/10.1101/2021.10.19.465059; this version posted October 20, 2021. The copyright holder for this preprint (which was not certified by peer review) is the author/funder, who has granted bioRxiv a license to display the preprint in perpetuity. It is made available under aCC-BY-NC-ND 4.0 International license.

The beneficial effects of *drp-1* disruption on mitochondrial morphology in Neur-67Q worms is also observed at day 7 of adulthood (**Fig 3A**). In Neur-67Q worms, disruption of *drp-1* increases mitochondrial number (**Fig. 3B**), increases mitochondrial area (**Fig. 3C**), increases axonal mitochondrial load (**Fig. 3D**), decreases mitochondrial circularity (**Fig. 3E**), and increases the Feret's diameter of the mitochondria (**Fig. 3F**). Similar changes are observed in wild-type worms with the exception of mitochondrial number, which is significantly decreased by *drp-1* disruption (**Fig. 3B**).

Combined, these results indicate that *drp-1* has a beneficial effect on mitochondrial morphology in Neur-67Q worms. Interestingly, CAG repeat expansion in Neur-67Q worms has no effect on mitochondrial morphology in the *drp-1* mutant background (**Fig. S7**).

Targeting genes that affect mitochondrial fragmentation improves thrashing rate and lifespan in a neuronal model of polyglutamine toxicity

While our results show that decreasing levels of *drp-1* are beneficial in a neuronal worm model of polyglutamine toxicity, this treatment had a detrimental effect in a *C. elegans* model of HD in which exon 1 of mutant huntingtin is expressed in the body wall muscle [23]. Moreover, a number of studies have found that disruption of DRP1 can be detrimental in organisms ranging from worms to humans [27-32].

To circumvent potential detrimental effects of disrupting *drp-1*, we targeted other genes that have been previously found to decrease mitochondrial fragmentation [44]. In the previous study, a targeted RNAi screen identified 24 mitochondria-related RNAi clones that decrease mitochondrial fragmentation in the body wall muscle of *C. elegans*. We examined the effect of these 24 RNAi clones in neuron-specific RNAi Neur-67Q worms (Neur-67Q*; sid-1; unc-119p::sid-1*). Treatment with RNAi was begun at the L4 stage of the parental generation, and the rate of movement was assessed in the progeny (experimental generation).

bioRxiv preprint doi: https://doi.org/10.1101/2021.10.19.465059; this version posted October 20, 2021. The copyright holder for this preprint (which was not certified by peer review) is the author/funder, who has granted bioRxiv a license to display the preprint in perpetuity. It is made available under aCC-BY-NC-ND 4.0 International license.

We found that 16 of the 24 RNAi clones that decrease mitochondrial fragmentation significantly increased the rate of movement in the neuron-specific RNAi Neur-67Q model (**Fig. 4A**). To ensure that the improved movement in Neur-67Q worms did not results from a general effect of these RNAi clones on the rate of movement, we treated *sid-1;unc-119p::sid-1* control worms with the same panel of 24 RNAi clones and examined movement. Unlike the Neur-67Q worms, we found that only four of the RNAi clones improved movement in the neuron-specific RNAi strain (**Fig. 4B**). This indicates that for the majority of the RNAi clones that show a benefit, the improvement in movement is specific to the neuronal model of polyglutamine toxicity.

We next examined whether the genes that improved motility in neuron-specific RNAi Neur-67Q worms also improved longevity. We found that 11 of the 16 RNAi clones that increased the rate of movement also increased lifespan in neuron-specific RNAi Neur-67Q worms (**Fig. 5**). In contrast, only 3 of these RNAi clones increased lifespan in the neuron-specific RNAi control strain (**Fig. S8**). Overall, RNAi clones which decrease mitochondrial fragmentation in body wall muscle are beneficial in a neuronal model of polyglutamine toxicity. The corresponding target genes represent novel therapeutic targets for HD and other polyglutamine toxicity disorders.

bioRxiv preprint doi: https://doi.org/10.1101/2021.10.19.465059; this version posted October 20, 2021. The copyright holder for this preprint (which was not certified by peer review) is the author/funder, who has granted bioRxiv a license to display the preprint in perpetuity. It is made available under aCC-BY-NC-ND 4.0 International license.

Discussion

Since the discovery of the genes responsible for HD and other polyglutamine toxicity disorders [45,46], multiple animal models of these disorders have been generated to gain insight into disease pathogenesis [47,48]. This includes *C. elegans* models of HD and polyglutamine toxicity [33,49-51]. *C. elegans* offers a number of advantages for studying neurodegenerative disease including being able to perform large scale screens for disease modifiers rapidly and cost effectively [52,53]. In addition, the interconnections of all of the neurons in *C. elegans* have been mapped. In terms of studying mitochondrial dynamics, the transparent nature of *C. elegans* facilitates imaging mitochondrial morphology in a live organism, which can then be correlated with whole organism phenotypes.

CAG repeat expansion disrupts mitochondrial morphology and function in neurons

HD and other polyglutamine toxicity disorders are neurodegenerative diseases in which the most severe pathology occurs in neurons. We previously examined mitochondrial fragmentation in a muscle model of HD as it is more experimentally accessible [23]. However, to gain greater physiological relevance, in this study, we generated novel strains to examine mitochondrial morphology in neurons. We found that CAG repeat expansion in Neur-67Q worms is sufficient to cause mitochondrial fragmentation neurons as well as a progressive decrease in the abundance of mitochondria in the axons of the dorsal nerve cord. The differences in mitochondrial number, axonal load, size, circularity and length (Feret's diameter) in the neuronal model of polyglutamine toxicity are quantifiable and highly significant.

Importantly, Neur-67Q worms also exhibited changes in mitochondrial function including a significant increase in oxygen consumption and a significant decrease in ATP levels. These differences are particularly striking given that oxygen consumption and ATP levels were measured in whole worms while the expanded polyglutamine transgene is only expressed in neurons, which make up 302 of the worm's 959 cells. Given the magnitude of the differences

bioRxiv preprint doi: https://doi.org/10.1101/2021.10.19.465059; this version posted October 20, 2021. The copyright holder for this preprint (which was not certified by peer review) is the author/funder, who has granted bioRxiv a license to display the preprint in perpetuity. It is made available under aCC-BY-NC-ND 4.0 International license.

observed, it is possible that changes occurring in the neurons are having cell-non-autonomous effects on mitochondrial function in other tissues.

Although the yield of ATP from oxidative phosphorylation is variable [54], oxygen consumption and ATP production normally correlate under basal conditions due to the high dependence of ATP production on the electron transport chain in *C. elegans* [55,56]. The opposing changes in ATP and oxygen consumption suggest that the mitochondria in Neur-67Q worms are inefficient or damaged, leading to a marked decrease in ATP produced per amount of oxygen consumed. We observed a similar pattern in a mitophagy-defective worm model of Parkinson's disease in which there is a deletion of *pdr-1/PRKN* [35].

Tissue-specific effects of disrupting mitochondrial fission

One of the most surprising findings of our current study is that deletion of *drp-1* has different effects in neuronal and body wall muscle models of polyglutamine toxicity (see **Table S1** for comparison). In the neuronal model, deletion of *drp-1* increases movement and lifespan and has no detrimental effect on development or fertility. In contrast, disruption of *drp-1* in the body wall muscle model decreases movement, lifespan, fertility and the rate of development [23]. The opposing effects of reducing *drp-1* on polyglutamine toxicity in neurons compared to body wall muscle suggest that the optimal balance between mitochondrial fission and fusion may differ between tissues. Alternatively, it is possible that the loss of mitochondrial fission is better tolerated in neurons than in body wall muscle, even though both tissues are post-mitotic. Finally, it could be that decreasing *drp-1* levels is beneficial in neurons because it is more effective at correcting disruptions in mitochondrial networks in that tissue (**Fig 3**) than in body wall muscle, where *drp-1* deletion had little or no effect on mitochondrial morphology [23].

It should be noted that the neuronal model of polyglutamine toxicity used in this study and the HD muscle model that we utilized previously cannot be directly compared due to differences between these strains beyond the tissue of expression. Notably, BW-Htt-74Q worms have a small fragment of the huntingtin protein linked to the expanded polyglutamine tract, while

bioRxiv preprint doi: https://doi.org/10.1101/2021.10.19.465059; this version posted October 20, 2021. The copyright holder for this preprint (which was not certified by peer review) is the author/funder, who has granted bioRxiv a license to display the preprint in perpetuity. It is made available under aCC-BY-NC-ND 4.0 International license.

Neur-67Q only have the expanded polyglutamine tract. The size of the polyglutamine tract is different between these two strains, and BW-Htt-74Q worms have the polyglutamine tagged with GFP, while the polyglutamine is tagged with YFP in Neur-67Q worms. Thus, while our results do not rule out other factors contributing to the differences between the neuronal strain and the muscle strain, they clearly show that decreasing *drp-1* levels can be beneficial in worms expressing an expanded polyglutamine tract in neurons, and that decreasing *drp-1* levels can be detrimental in worms expressing an expanded polyglutamine tract in muscle cells.

Decreasing mitochondrial fragmentation as a therapeutic strategy for polyglutamine toxicity disorders

Due to the many roles *drp-1* plays in promoting proper cellular function through control of the mitochondria and the previously observed detrimental effects of decreasing *drp-1* in a body wall muscle model [23], decreasing levels or activity of DRP-1 may be a non-ideal therapeutic target for HD or other polyglutamine toxicity disorders. Accordingly, we explored other possible genetic targets that decrease mitochondrial fragmentation. We performed a targeted RNAi screen using 24 RNAi clones previously found to decrease mitochondrial fragmentation in body wall muscle [44]. A high percentage of these RNAi clones increased movement (16 of 24 RNAi clones that decrease fragmentation) and lifespan (11 of 16 RNAi clones that improve movement) in Neur-67Q worms.

As we obtained numerous positive hits, we did not confirm knockdown by qPCR or confirm a decrease in mitochondrial fragmentation. Thus, we can't exclude the possibility that the remaining eight genes that failed to show a beneficial effect may have had either insufficient genetic knockdown or did not exhibit the predicted effect on mitochondrial morphology. Nonetheless, a high proportion of RNAi clones previously found to decrease mitochondrial fragmentation increased movement in the neuronal HD model indicating that multiple genetic approaches to decreasing mitochondrial fragmentation are beneficial in worm models of polyglutamine toxicity.

bioRxiv preprint doi: https://doi.org/10.1101/2021.10.19.465059; this version posted October 20, 2021. The copyright holder for this preprint (which was not certified by peer review) is the author/funder, who has granted bioRxiv a license to display the preprint in perpetuity. It is made available under aCC-BY-NC-ND 4.0 International license.

In order to prioritize therapeutic targets for further characterization and validation, we analyzed the results from the current study with our previous study of these RNAi clones in a body wall muscle model of HD [23] (**Table 1**). The genes were ranked by giving one point for improving either: thrashing rate in Neur-67Q worms; lifespan in Neur-67Q worms; crawling rate in BW-Htt74Q worms; or thrashing rate in BW-Htt74Q worms. Of the 24 RNAi clones tested in both models, 21 clones exhibited a beneficial effect on at least one phenotype. This indicates that multiple approaches to decreasing mitochondrial fragmentation can ameliorate deficits caused by CAG repeat expansion. The top-ranked therapeutic targets were *alh-12* and *pgp-3*, which resulted in improvement of all four assessments, and *gpd-4, immt-2, sdha-2* and *wht-1*, which resulted in improvement in three of the assessments (**Table 1**).

alh-12 encodes a cytoplasmic aldehyde dehydrogenase that is expressed in the intestine, body wall muscle and specific neurons. It is involved in multiple metabolic pathways including arginine metabolism, glycerolipid metabolism, glycolysis/gluconeogenesis and tryptophan degradation. As very little is known about the functions of ALH-12, it is hard to speculate how disrupting *alh-12* may be acting to improve movement and lifespan in the worm models of polyglutamine toxicity.

pgp-3 encodes a p-glycoprotein related protein. It is a transmembrane protein that transports molecules out of the cytoplasm. PGP-3 is primarily expressed in the intestine [57], but has also been reported in other tissues. Disruption of *pgp-3* sensitizes worms to *P. aeruginosa* in a toxin-based fast kill assay [58] as well as exposure to colchicine and chloroquinone [59], presumably by disrupting the active removal of the toxic compounds from cells. It is unclear how loss of a protective function against toxins and xenobiotics is protective against polyglutamine toxicity, but it may be through hormesis, the process by which exposure to a mild stress activates protective pathways that can increase resistance to subsequent stresses and extend longevity.

bioRxiv preprint doi: https://doi.org/10.1101/2021.10.19.465059; this version posted October 20, 2021. The copyright holder for this preprint (which was not certified by peer review) is the author/funder, who has granted bioRxiv a license to display the preprint in perpetuity. It is made available under aCC-BY-NC-ND 4.0 International license.

Conclusions

In this work, we show that a *C. elegans* neuronal model of polyglutamine toxicity exhibit deficits in mitochondrial morphology and function, which are associated with decreased movement and lifespan. Decreasing the levels of the mitochondrial fission gene *drp-1* through genetic deletion or RNAi increases both movement and lifespan in Neur-67Q worms. Similarly, treatment of Neur-67Q worms with RNAi clones that decrease mitochondrial fragmentation resulted in increased movement and lifespan. Overall, this work suggests that decreasing mitochondrial fragmentation may be beneficial in treating HD and other polyglutamine toxicity disorders and identifies alternative genetic targets that circumvent the negative effects of disrupting DRP-1. Future studies will be needed to further investigate the mechanisms by which the genes we identified are beneficial and to validate these targets in other models of HD.

bioRxiv preprint doi: https://doi.org/10.1101/2021.10.19.465059; this version posted October 20, 2021. The copyright holder for this preprint (which was not certified by peer review) is the author/funder, who has granted bioRxiv a license to display the preprint in perpetuity. It is made available under aCC-BY-NC-ND 4.0 International license.

Author Contributions: Annika Traa: Conceptualization, Methodology, Validation, Formal analysis, Investigation, Visualization, Writing – review and editing. **Emily Machiela:** Conceptualization, Methodology, Validation, Formal analysis, Investigation, Writing – original draft, Visualization, Writing – review and editing. **Paige Rudich:** Conceptualization, Methodology, Validation, Formal analysis, Investigation, Visualization, Writing – review and editing, Supervision. **Sonja Soo:** Methodology, Validation, Formal analysis, Investigation, Visualization, Writing – review and editing. **Megan Senchuk:** Writing – review and editing, Supervision. **Jeremy Van Raamsdonk:** Conceptualization, Methodology, Validation, Formal analysis, Investigation, Visualization, Writing – original draft, Writing – review and editing, Supervision.

Conflict of Interests: The authors declare no conflicting interests.

Funding: This work was supported by the Canadian Institutes of Health Research (CIHR; http://www.cihr-irsc.gc.ca/; JVR), the Natural Sciences and Engineering Research Council of Canada (NSERC; https://www.nserc-crsng.gc.ca/index_eng.asp; JVR), the National Institute of General Medical Sciences (NIGMS; https://www.nigms.nih.gov/; JVR) by grant number R01 GM121756 and the Van Andel Research Institute (VARI). JVR is the recipient of a Senior Research Scholar career award from the Fonds de Recherche du Québec Santé (FRQS) and Parkinson Quebec. AT received scholarships from NSERC and FRQS. SKS received a scholarship from FRQS. PDR received a fellowship award from FRQS. The funders had no role in study design, data collection and analysis, decision to publish, or preparation of the manuscript.

Acknowledgements: Some strains were provided by the *Caenorhabditis* Genetics Center (CGC), which is funded by the National Institutes of Health (NIH) Office of Research Infrastructure Programs (P40 OD010440). We would also like to acknowledge the *C. elegans* knockout consortium and the National Bioresource Project of Japan for providing strains used in this research.

bioRxiv preprint doi: https://doi.org/10.1101/2021.10.19.465059; this version posted October 20, 2021. The copyright holder for this preprint (which was not certified by peer review) is the author/funder, who has granted bioRxiv a license to display the preprint in perpetuity. It is made available under aCC-BY-NC-ND 4.0 International license.

References

1. Zoghbi HY, Orr HT. Glutamine repeats and neurodegeneration. *Annual review of neuroscience.* 2000;23:217-247.
2. Lieberman AP, Shakkottai VG, Albin RL. Polyglutamine Repeats in Neurodegenerative Diseases. *Annual review of pathology.* 2019;14:1-27.
3. Lee JM, Galkina EI, Levantovsky RM, et al. Dominant effects of the Huntington's disease HTT CAG repeat length are captured in gene-expression data sets by a continuous analysis mathematical modeling strategy. *Human molecular genetics.* 2013;22(16):3227-3238.
4. Lee JM, Ramos EM, Lee JH, et al. CAG repeat expansion in Huntington disease determines age at onset in a fully dominant fashion. *Neurology.* 2012;78(10):690-695.
5. Costa V, Scorrano L. Shaping the role of mitochondria in the pathogenesis of Huntington's disease. *EMBO J.* 2012;31(8):1853-1864.
6. Oliveira JM. Nature and cause of mitochondrial dysfunction in Huntington's disease: focusing on huntingtin and the striatum. *Journal of neurochemistry.* 2010;114(1):1-12.
7. Browne SE, Bowling AC, MacGarvey U, et al. Oxidative damage and metabolic dysfunction in Huntington's disease: selective vulnerability of the basal ganglia. *Annals of neurology.* 1997;41(5):646-653.
8. Jenkins BG, Koroshetz WJ, Beal MF, Rosen BR. Evidence for impairment of energy metabolism in vivo in Huntington's disease using localized 1H NMR spectroscopy. *Neurology.* 1993;43(12):2689-2695.
9. Seong IS, Ivanova E, Lee JM, et al. HD CAG repeat implicates a dominant property of huntingtin in mitochondrial energy metabolism. *Human molecular genetics.* 2005;14(19):2871-2880.
10. Panov AV, Gutekunst CA, Leavitt BR, et al. Early mitochondrial calcium defects in Huntington's disease are a direct effect of polyglutamines. *Nature neuroscience.* 2002;5(8):731-736.
11. Trushina E, Dyer RB, Badger JD, 2nd, et al. Mutant huntingtin impairs axonal trafficking in mammalian neurons in vivo and in vitro. *Molecular and cellular biology.* 2004;24(18):8195-8209.
12. Ferro A, Carbone E, Zhang J, et al. Short-term succinic acid treatment mitigates cerebellar mitochondrial OXPHOS dysfunction, neurodegeneration and ataxia in a Purkinje-specific spinocerebellar ataxia type 1 (SCA1) mouse model. *PLoS One.* 2017;12(12):e0188425.
13. Kazachkova N, Raposo M, Montiel R, et al. Patterns of mitochondrial DNA damage in blood and brain tissues of a transgenic mouse model of Machado-Joseph disease. *Neuro-degenerative diseases.* 2013;11(4):206-214.
14. Giorgetti E, Yu Z, Chua JP, et al. Rescue of Metabolic Alterations in AR113Q Skeletal Muscle by Peripheral Androgen Receptor Gene Silencing. *Cell reports.* 2016;17(1):125-136.
15. Rocchi A, Milioto C, Parodi S, et al. Glycolytic-to-oxidative fiber-type switch and mTOR signaling activation are early-onset features of SBMA muscle modified by high-fat diet. *Acta neuropathologica.* 2016;132(1):127-144.

bioRxiv preprint doi: https://doi.org/10.1101/2021.10.19.465059; this version posted October 20, 2021. The copyright holder for this preprint (which was not certified by peer review) is the author/funder, who has granted bioRxiv a license to display the preprint in perpetuity. It is made available under aCC-BY-NC-ND 4.0 International license.

16. Wang H, Lim PJ, Karbowski M, Monteiro MJ. Effects of overexpression of huntingtin proteins on mitochondrial integrity. *Hum Mol Genet.* 2009;18(4):737-752.
17. Song W, Chen J, Petrilli A, et al. Mutant huntingtin binds the mitochondrial fission GTPase dynamin-related protein-1 and increases its enzymatic activity. *Nature medicine.* 2011;17(3):377-382.
18. Haun F, Nakamura T, Shiu AD, et al. S-nitrosylation of dynamin-related protein 1 mediates mutant huntingtin-induced mitochondrial fragmentation and neuronal injury in Huntington's disease. *Antioxidants & redox signaling.* 2013;19(11):1173-1184.
19. Guo X, Disatnik MH, Monbureau M, Shamloo M, Mochly-Rosen D, Qi X. Inhibition of mitochondrial fragmentation diminishes Huntington's disease-associated neurodegeneration. *The Journal of clinical investigation.* 2013;123(12):5371-5388.
20. Jin YN, Yu YV, Gundemir S, et al. Impaired mitochondrial dynamics and Nrf2 signaling contribute to compromised responses to oxidative stress in striatal cells expressing full-length mutant huntingtin. *PloS one.* 2013;8(3):e57932.
21. Joshi AU, Ebert AE, Haileselassie B, Mochly-Rosen D. Drp1/Fis1-mediated mitochondrial fragmentation leads to lysosomal dysfunction in cardiac models of Huntington's disease. *J Mol Cell Cardiol.* 2019;127:125-133.
22. Costa V, Giacomello M, Hudec R, et al. Mitochondrial fission and cristae disruption increase the response of cell models of Huntington's disease to apoptotic stimuli. *EMBO molecular medicine.* 2010;2(12):490-503.
23. Machiela E, Rudich PD, Traa A, et al. Targeting Mitochondrial Network Disorganization is Protective in C. elegans Models of Huntington's Disease. *Aging and disease.* 2021;Epub:0-.
24. Borgia D, Malena A, Spinazzi M, et al. Increased mitophagy in the skeletal muscle of spinal and bulbar muscular atrophy patients. *Hum Mol Genet.* 2017;26(6):1087-1103.
25. Harmuth T, Prell-Schicker C, Weber JJ, et al. Mitochondrial Morphology, Function and Homeostasis Are Impaired by Expression of an N-terminal Calpain Cleavage Fragment of Ataxin-3. *Frontiers in molecular neuroscience.* 2018;11:368.
26. Ward JM, Stoyas CA, Switonski PM, et al. Metabolic and Organelle Morphology Defects in Mice and Human Patients Define Spinocerebellar Ataxia Type 7 as a Mitochondrial Disease. *Cell reports.* 2019;26(5):1189-1202 e1186.
27. Ishihara N, Nomura M, Jofuku A, et al. Mitochondrial fission factor Drp1 is essential for embryonic development and synapse formation in mice. *Nature cell biology.* 2009;11(8):958-966.
28. Waterham HR, Koster J, van Roermund CW, Mooyer PA, Wanders RJ, Leonard JV. A lethal defect of mitochondrial and peroxisomal fission. *The New England journal of medicine.* 2007;356(17):1736-1741.
29. Wakabayashi J, Zhang Z, Wakabayashi N, et al. The dynamin-related GTPase Drp1 is required for embryonic and brain development in mice. *The Journal of cell biology.* 2009;186(6):805-816.
30. Byrne JJ, Soh MS, Chandhok G, et al. Disruption of mitochondrial dynamics affects behaviour and lifespan in Caenorhabditis elegans. *Cell Mol Life Sci.* 2019;76(10):1967-1985.

bioRxiv preprint doi: https://doi.org/10.1101/2021.10.19.465059; this version posted October 20, 2021. The copyright holder for this preprint (which was not certified by peer review) is the author/funder, who has granted bioRxiv a license to display the preprint in perpetuity. It is made available under aCC-BY-NC-ND 4.0 International license.

31. Fahrner JA, Liu R, Perry MS, Klein J, Chan DC. A novel de novo dominant negative mutation in DNM1L impairs mitochondrial fission and presents as childhood epileptic encephalopathy. *Am J Med Genet A.* 2016;170(8):2002-2011.
32. Machiela E, Liontis T, Dues DJ, et al. Disruption of mitochondrial dynamics increases stress resistance through activation of multiple stress response pathways. *FASEB journal : official publication of the Federation of American Societies for Experimental Biology.* 2020;34(6):8475-8492.
33. Brignull HR, Moore FE, Tang SJ, Morimoto RI. Polyglutamine proteins at the pathogenic threshold display neuron-specific aggregation in a pan-neuronal Caenorhabditis elegans model. *J Neurosci.* 2006;26(29):7597-7606.
34. El Mouridi S, Lecroisey C, Tardy P, et al. Reliable CRISPR/Cas9 Genome Engineering in Caenorhabditis elegans Using a Single Efficient sgRNA and an Easily Recognizable Phenotype. *G3.* 2017;7(5):1429-1437.
35. Cooper JF, Machiela E, Dues DJ, Spielbauer KK, Senchuk MM, Van Raamsdonk JM. Activation of the mitochondrial unfolded protein response promotes longevity and dopamine neuron survival in Parkinson's disease models. *Scientific reports.* 2017;7(1):16441.
36. Wu Z, Senchuk MM, Dues DJ, et al. Mitochondrial unfolded protein response transcription factor ATFS-1 promotes longevity in a long-lived mitochondrial mutant through activation of stress response pathways. *BMC biology.* 2018;16(1):147.
37. Cooper JF, Dues DJ, Spielbauer KK, Machiela E, Senchuk MM, Van Raamsdonk JM. Delaying aging is neuroprotective in Parkinson's disease: a genetic analysis in C. elegans models. *NPJ Parkinson's disease.* 2015;1:15022.
38. Van Raamsdonk JM, Hekimi S. FUdR causes a twofold increase in the lifespan of the mitochondrial mutant gas-1. *Mech Ageing Dev.* 2011;132(10):519-521.
39. Schaar CE, Dues DJ, Spielbauer KK, et al. Mitochondrial and cytoplasmic ROS have opposing effects on lifespan. *PLoS Genet.* 2015;11(2):e1004972.
40. Machiela E, Dues DJ, Senchuk MM, Van Raamsdonk JM. Oxidative stress is increased in C. elegans models of Huntington's disease but does not contribute to polyglutamine toxicity phenotypes. *Neurobiology of disease.* 2016;96:1-11.
41. Senchuk MM, Dues DJ, Schaar CE, et al. Activation of DAF-16/FOXO by reactive oxygen species contributes to longevity in long-lived mitochondrial mutants in Caenorhabditis elegans. *PLoS Genet.* 2018;14(3):e1007268.
42. Firnhaber C, Hammarlund M. Neuron-specific feeding RNAi in C. elegans and its use in a screen for essential genes required for GABA neuron function. *PLoS Genet.* 2013;9(11):e1003921.
43. Calixto A, Chelur D, Topalidou I, Chen X, Chalfie M. Enhanced neuronal RNAi in C. elegans using SID-1. *Nature methods.* 2010;7(7):554-559.
44. Ichishita R, Tanaka K, Sugiura Y, Sayano T, Mihara K, Oka T. An RNAi screen for mitochondrial proteins required to maintain the morphology of the organelle in Caenorhabditis elegans. *Journal of biochemistry.* 2008;143(4):449-454.
45. Huntington's Study Group. A novel gene containing a trinucleotide repeat that is expanded and unstable on Huntington's disease chromosomes. The Huntington's Disease Collaborative Research Group. *Cell.* 1993;72(6):971-983.

bioRxiv preprint doi: https://doi.org/10.1101/2021.10.19.465059; this version posted October 20, 2021. The copyright holder for this preprint (which was not certified by peer review) is the author/funder, who has granted bioRxiv a license to display the preprint in perpetuity. It is made available under aCC-BY-NC-ND 4.0 International license.

631 46. Banfi S, Servadio A, Chung MY, et al. Identification and characterization of the gene
632 causing type 1 spinocerebellar ataxia. *Nature genetics.* 1994;7(4):513-520.
633 47. Slow EJ, van Raamsdonk J, Rogers D, et al. Selective striatal neuronal loss in a YAC128
634 mouse model of Huntington disease. *Human molecular genetics.* 2003;12(13):1555-
635 1567.
636 48. Mangiarini L, Sathasivam K, Seller M, et al. Exon 1 of the HD gene with an expanded CAG
637 repeat is sufficient to cause a progressive neurological phenotype in transgenic mice.
638 *Cell.* 1996;87(3):493-506.
639 49. Morley JF, Brignull HR, Weyers JJ, Morimoto RI. The threshold for polyglutamine-
640 expansion protein aggregation and cellular toxicity is dynamic and influenced by aging in
641 Caenorhabditis elegans. *Proc Natl Acad Sci U S A.* 2002;99(16):10417-10422.
642 50. Wang H, Lim PJ, Yin C, Rieckher M, Vogel BE, Monteiro MJ. Suppression of
643 polyglutamine-induced toxicity in cell and animal models of Huntington's disease by
644 ubiquilin. *Hum Mol Genet.* 2006;15(6):1025-1041.
645 51. Parker JA, Connolly JB, Wellington C, Hayden M, Dausset J, Neri C. Expanded
646 polyglutamines in Caenorhabditis elegans cause axonal abnormalities and severe
647 dysfunction of PLM mechanosensory neurons without cell death. *Proc Natl Acad Sci U S*
648 *A.* 2001;98(23):13318-13323.
649 52. Nollen EA, Garcia SM, van Haaften G, et al. Genome-wide RNA interference screen
650 identifies previously undescribed regulators of polyglutamine aggregation. *Proc Natl*
651 *Acad Sci U S A.* 2004;101(17):6403-6408.
652 53. Lejeune FX, Mesrob L, Parmentier F, et al. Large-scale functional RNAi screen in C.
653 elegans identifies genes that regulate the dysfunction of mutant polyglutamine neurons.
654 *BMC genomics.* 2012;13:91.
655 54. Salin K, Auer SK, Rey B, Selman C, Metcalfe NB. Variation in the link between oxygen
656 consumption and ATP production, and its relevance for animal performance. *Proc Biol*
657 *Sci.* 2015;282(1812):20151028.
658 55. Bratic I, Trifunovic A. Mitochondrial energy metabolism and ageing. *Biochimica et*
659 *biophysica acta.* 2010;1797(6-7):961-967.
660 56. Lemire BD, Behrendt M, DeCorby A, Gaskova D. C. elegans longevity pathways converge
661 to decrease mitochondrial membrane potential. *Mech Ageing Dev.* 2009;130(7):461-
662 465.
663 57. Lincke CR, Broeks A, The I, Plasterk RH, Borst P. The expression of two P-glycoprotein
664 (pgp) genes in transgenic Caenorhabditis elegans is confined to intestinal cells. *The*
665 *EMBO journal.* 1993;12(4):1615-1620.
666 58. Mahajan-Miklos S, Tan MW, Rahme LG, Ausubel FM. Molecular mechanisms of bacterial
667 virulence elucidated using a Pseudomonas aeruginosa-Caenorhabditis elegans
668 pathogenesis model. *Cell.* 1999;96(1):47-56.
669 59. Broeks A, Janssen HW, Calafat J, Plasterk RH. A P-glycoprotein protects Caenorhabditis
670 elegans against natural toxins. *The EMBO journal.* 1995;14(9):1858-1866.

671

672

bioRxiv preprint doi: https://doi.org/10.1101/2021.10.19.465059; this version posted October 20, 2021. The copyright holder for this preprint (which was not certified by peer review) is the author/funder, who has granted bioRxiv a license to display the preprint in perpetuity. It is made available under aCC-BY-NC-ND 4.0 International license.

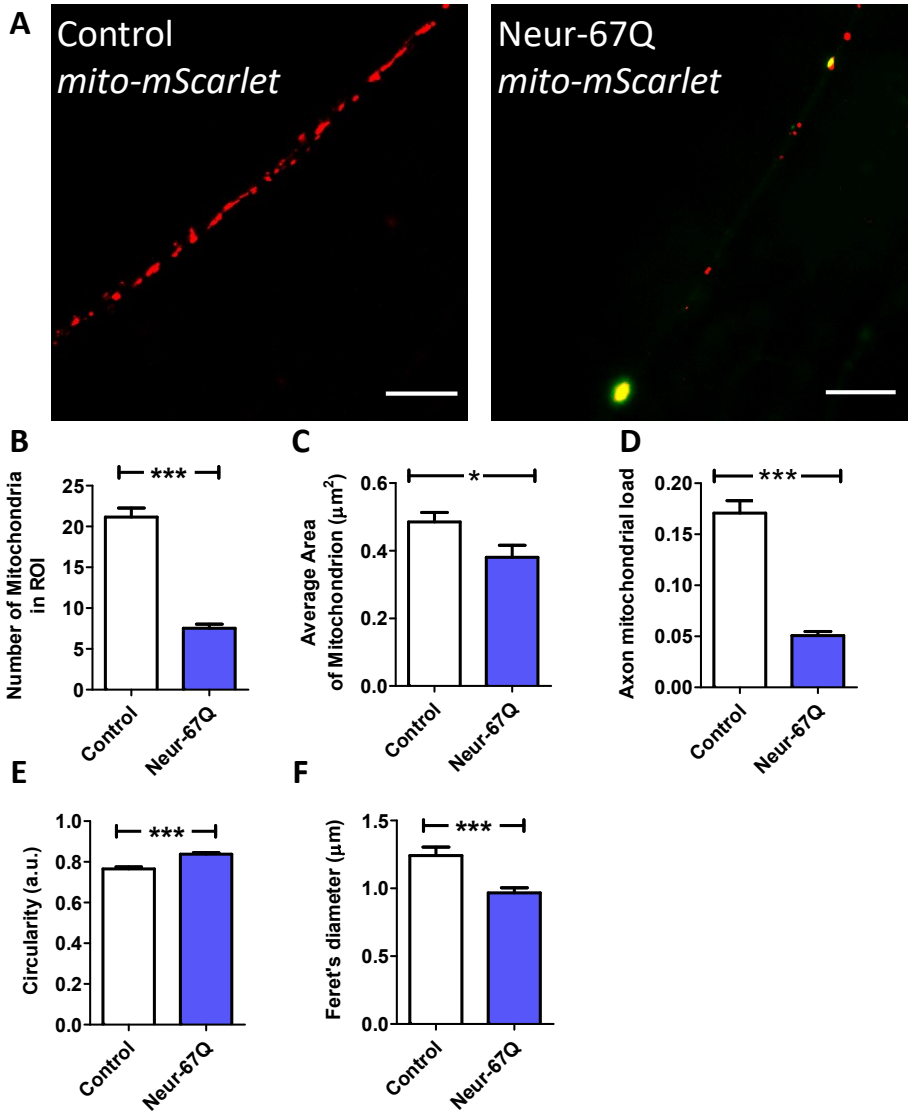

Figure 1. CAG repeat expansion disrupts mitochondrial morphology in neurons. Representative images of mitochondria (red) in dorsal nerve cord in control and Neur-67Q worms at day 7 of adulthood demonstrate that Neur-67Q worms exhibit mitochondrial fragmentation and decreased numbers of mitochondria in neurons (**A**). Mitochondrial morphology was visualized by fusing the red fluorescent protein mScarlet to the mitochondrially-targeted protein TOMM-20 in order to target mScarlet to the mitochondria. Quantification of mitochondrial morphology reveals that Neur-67Q worms have a significantly decreased number of mitochondria compared to control worms (**B**). Neur-67Q worms also exhibit decreased mitochondrial area (**C**), decreased axonal mitochondrial load (**D**), increased mitochondrial circularity (**E**) and a decreased mitochondrial Feret's diameter (**F**) compared to control worms. Control worms are *rab-3p::tomm-20::mScarlet.* Three biological replicates were performed. Statistical significance was assessed using a t-test. Error bar indicate SEM. *p<0.05, ***p<0.001.

bioRxiv preprint doi: https://doi.org/10.1101/2021.10.19.465059; this version posted October 20, 2021. The copyright holder for this preprint (which was not certified by peer review) is the author/funder, who has granted bioRxiv a license to display the preprint in perpetuity. It is made available under aCC-BY-NC-ND 4.0 International license.

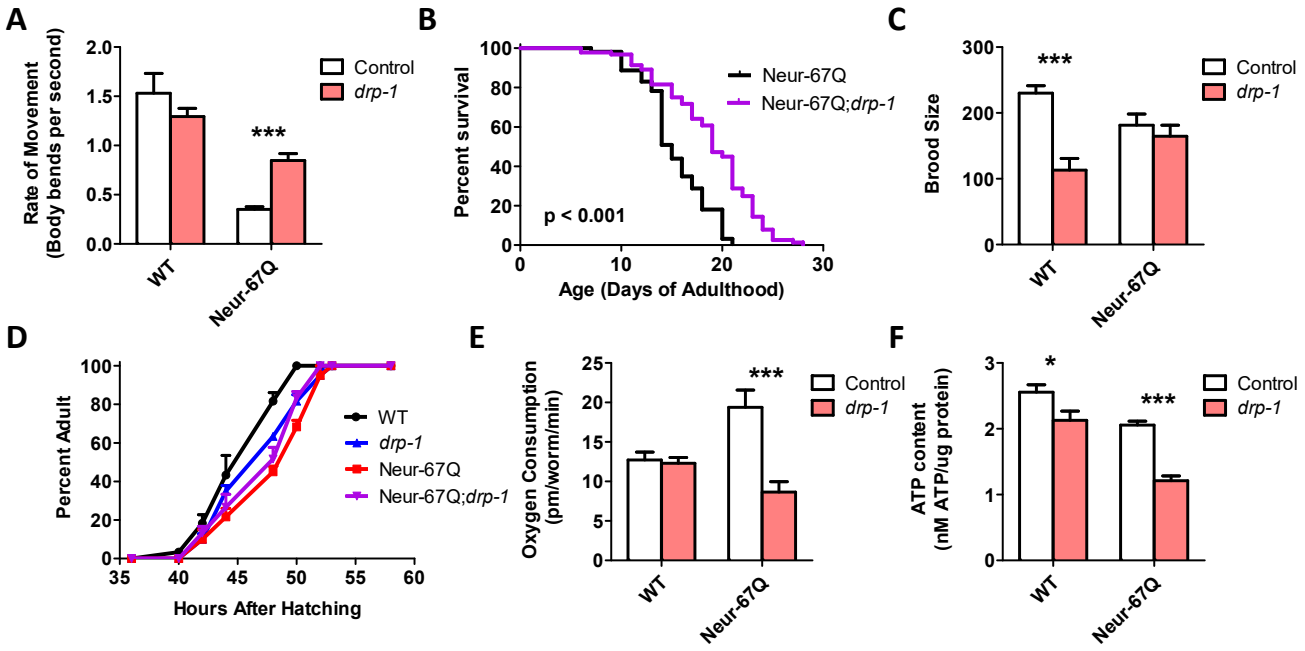

Figure 2. Inhibition of mitochondrial fission is beneficial in a neuronal model of polyglutamine toxicity. To examine the effect of disrupting mitochondrial fission in a neuronal model of polyglutamine toxicity, Neur-67Q worms were crossed to *drp-1* deletion mutants. Deletion of *drp-1* partially ameliorated phenotypic deficits in Neur-67Q worms. Neur-67Q;*drp-1* worms showed significantly increased movement (**A**) and lifespan (**B**) compared to Neur-67Q worms. Unlike wild-type worms, deletion of *drp-1* did not decrease fertility (**C**) or development time (**D**) in Neur-67Q worms. Combined this indicates that inhibiting mitochondrial fission is beneficial in a neuronal model of polyglutamine toxicity. Neur-67Q worms have increased oxygen consumption compared to wild-type worms, and a mutation in *drp-1* decreases oxygen consumption in these worms (**E**). Deletion of *drp-1* causes a decrease in ATP levels in both wild-type and Neur-67Q worms (**F**). Control data for wild-type and *drp-1* worms was previously published in Machiela et al., 2021 as experiments for both papers were performed simultaneously using the same controls. A minimum of three biological replicates were performed. Statistical significance was assessed using a two-way ANOVA with Bonferroni posttest (panels A,C,E,F), the log-rank test (panel B) or a repeated measures ANOVA (panel D). Error bars indicate SEM. *p<0.05, ***p<0.001.

bioRxiv preprint doi: https://doi.org/10.1101/2021.10.19.465059; this version posted October 20, 2021. The copyright holder for this preprint (which was not certified by peer review) is the author/funder, who has granted bioRxiv a license to display the preprint in perpetuity. It is made available under aCC-BY-NC-ND 4.0 International license.

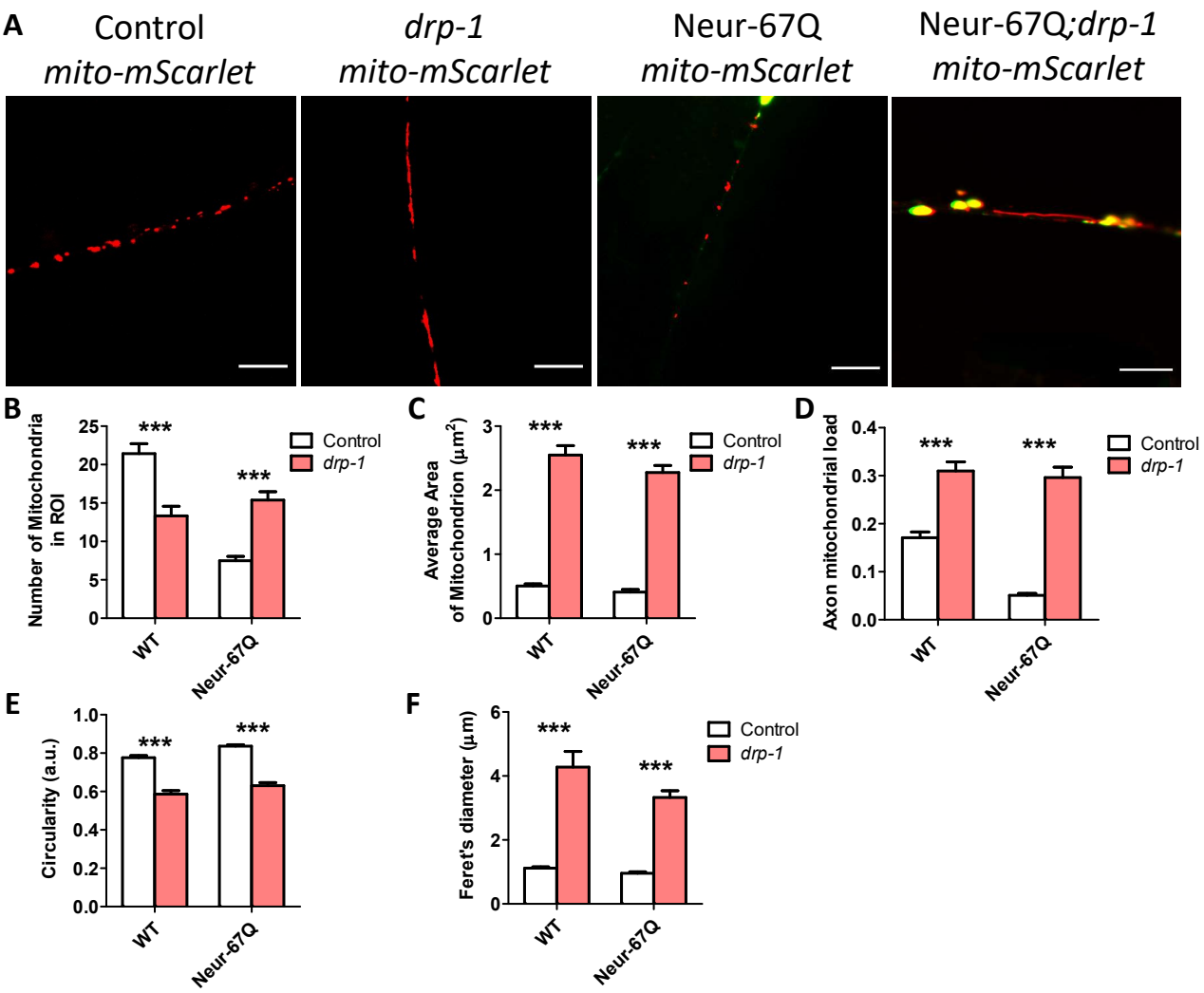

Figure 3. Disruption of *drp-1* rescues deficits in mitochondrial morphology caused by CAG repeat expansion. Deletion of *drp-1* decreased mitochondrial fragmentation in Neur-67Q and control worms at day 7 of adulthood. Representative images of Neur-67Q worms and control worms in wild-type and *drp-1* deletion background (**A**). Disruption of *drp-1* in Neur-67Q worms increased mitochondrial number (**B**), increased mitochondrial area (**C**), increased axonal mitochondrial load (**D**), decreased mitochondrial circularity (**E**), and increased the Feret's diameter of the mitochondria (**F**). Control worms are *rab-3p::tomm-20::mScarlet.* Three biological replicates were performed. Statistical significance was assessed using a two-way ANOVA with Bonferroni posttest. Error bars indicate SEM. ***p<0.001.

bioRxiv preprint doi: https://doi.org/10.1101/2021.10.19.465059; this version posted October 20, 2021. The copyright holder for this preprint (which was not certified by peer review) is the author/funder, who has granted bioRxiv a license to display the preprint in perpetuity. It is made available under aCC-BY-NC-ND 4.0 International license.

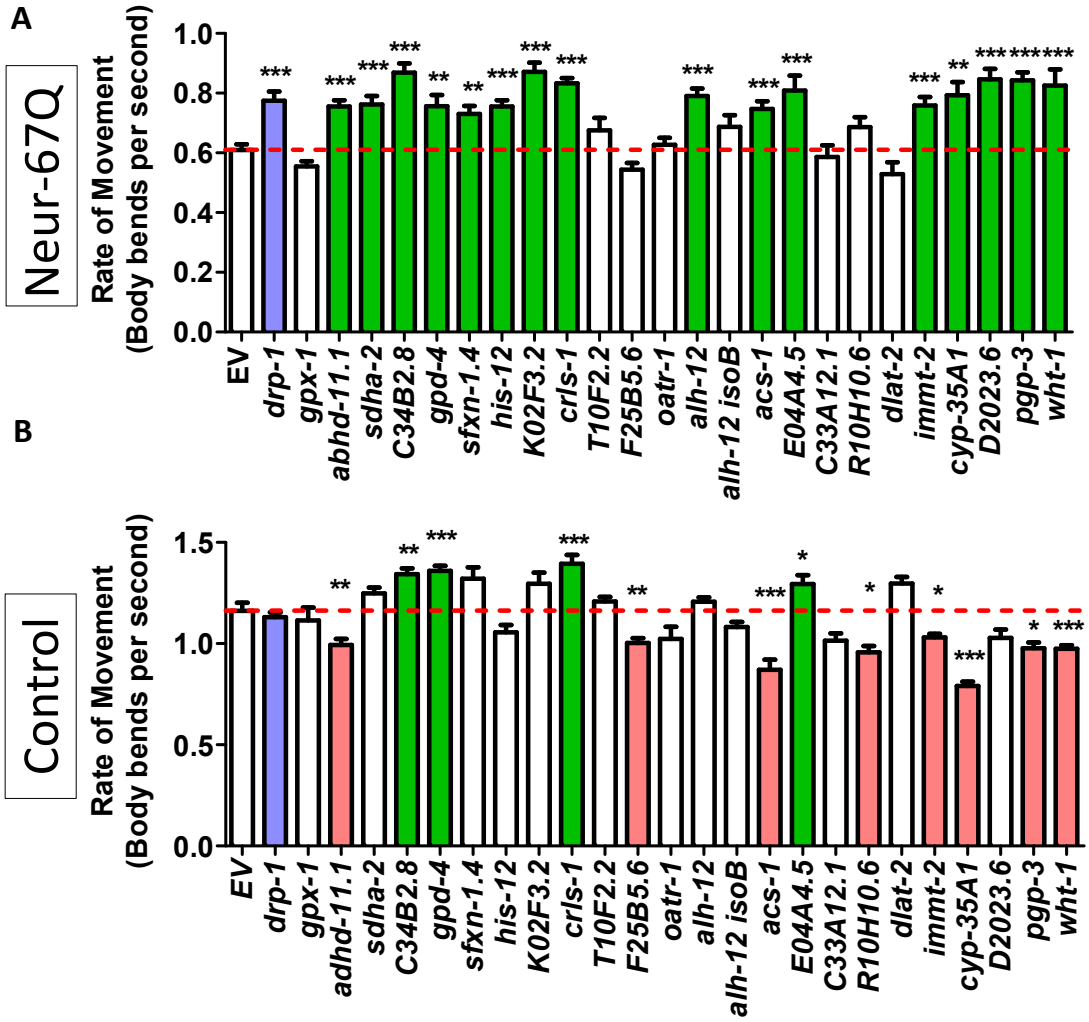

Figure 4. Decreasing mitochondrial fragmentation improves rate of movement in a neuronal model of polyglutamine toxicity. Neur-67Q worms in which RNAi is only effective in neurons (Neur-67Q*;sid-1;unc-119p::sid-1* worms) and a neuron-specific RNAi control strain (*sid-1;unc-119p::sid-1* worms) were treated with RNAi clones that decrease mitochondrial fragmentation. RNAi against 16 of the 24 genes tested improved the rate of movement in Neur-67Q worms (**A**). RNAi against four of these genes also increased movement in the neuron specific RNAi strain (**B**). Green indicates a significant increase in movement, while red indicates a significant decrease in movement. The positive control *drp-1* is indicated with blue. Three biological replicates were performed. Statistical significance was assessed using a one-way ANOVA with Dunnett's multiple comparison test. Error bars indicate SEM. **p*<0.05, ***p*<0.01, ****p*<0.001.

bioRxiv preprint doi: https://doi.org/10.1101/2021.10.19.465059; this version posted October 20, 2021. The copyright holder for this preprint (which was not certified by peer review) is the author/funder, who has granted bioRxiv a license to display the preprint in perpetuity. It is made available under aCC-BY-NC-ND 4.0 International license.

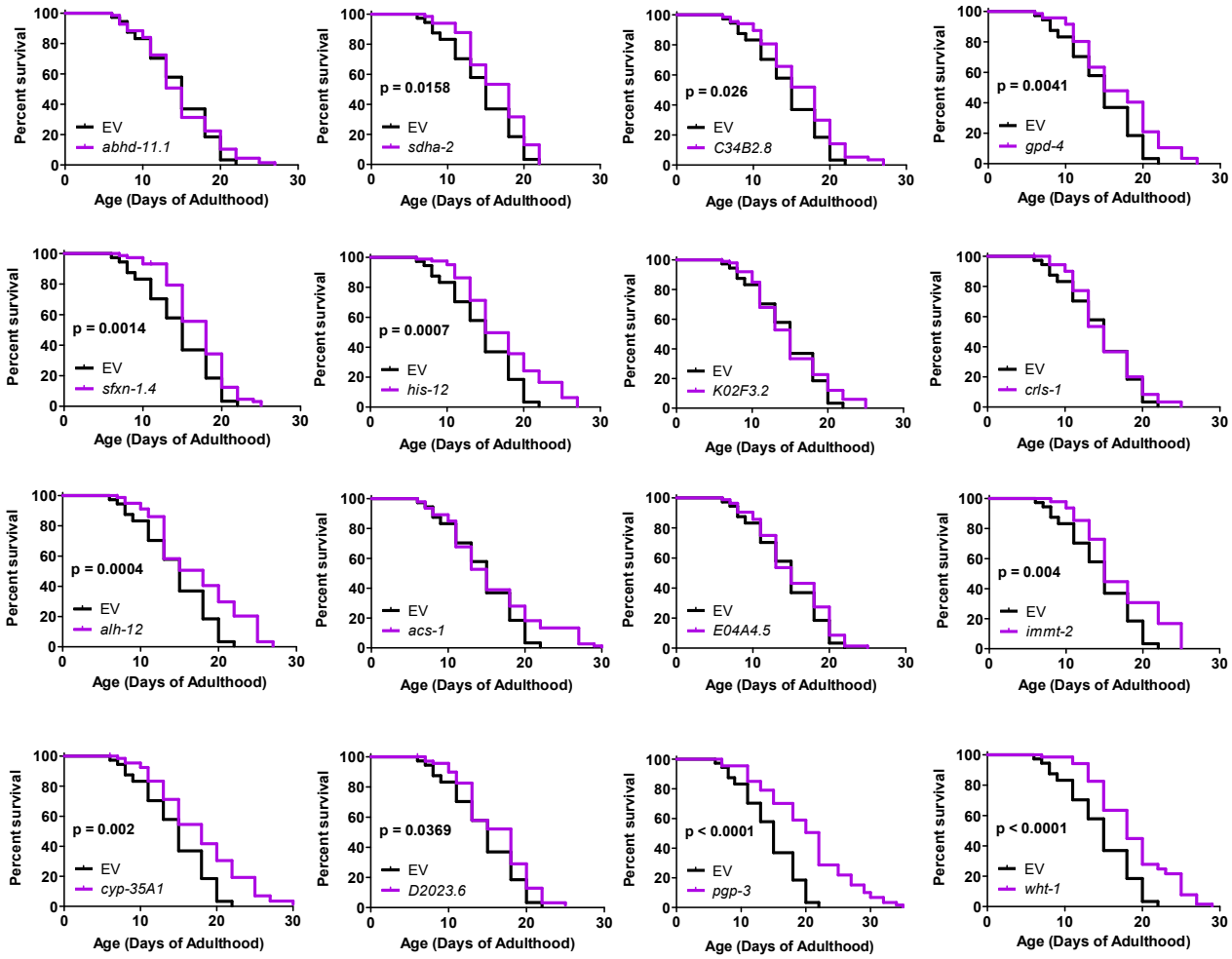

Figure 5. RNAi clones previously shown to decrease mitochondrial fragmentation in body wall muscle rescue shortened lifespan in neuronal model of polyglutamine toxicity. Neur-67Q worms in which RNAi is only effective in neurons (Neur-67Q*;sid-1;unc-119p::sid-1* worms) were treated with RNAi clones that decrease mitochondrial fragmentation and that we found to increase movement in Neur-67Q worms (Figure 4). Eleven of the sixteen RNAi clones that improved movement in Neur-67Q worms also resulted in increased lifespan. Three biological replicates were performed. Statistical significance was assessed using the log-rank test.

Table 1. Effect of RNAi clones that decrease mitochondrial fragmentation in neuronal and body wall muscle models of polyglutamine toxicity.
"ND" indicates not done. "=" indicates no change.

Target gene	*Drosophila* homolog	Mammalian homolog	Effect on thrashing in Neur-67Q worms	Effect on lifespan in Neur-67Q worms	Effect on crawling in BW-Htt74Q worms	Effect on thrashing in BW-Htt74Q worms	Effect on thrashing in neuron specific RNAi strain	Effect on lifespan in neuron specific RNAi strain	Effect of crawling in BW-Htt28Q worms	Effect of thrashing in BW-Htt28Q worms
alh-12	*Aldh*	*ALDH9A1*	Increased	Increased	Increased	Increased	No effect	Decreased	No effect	Decreased
pgp-3	*Mdr49*	*ABCB4*	Increased	Increased	Increased	Increased	Decreased	Increased	No effect	Decreased
gpd-4	*Gapdh2*	*GAPDH*	Increased	Increased	Increased	No effect	Increased	No effect	No effect	Decreased
immt-2	*Mitofilin*	*IMMT*	Increased	Increased	No effect	Increased	Decreased	Increased	No effect	No effect
sdha-2	*SdhA*	*SdhA*	Increased	Increased	Increased	No effect	No effect	Increased	Increased	Decreased
wht-1	*w*	*ABCG1*	Increased	Increased	Increased	No effect	Decreased	Decreased	No effect	No effect
C34B2.8	*ND-B16.6*	*NDUFA13*	Increased	Increased	Increased	Decreased	Increased	No effect	No effect	No effect
drp-1	*Drp1*	*DNM1L*	Increased	Increased	No effect	No effect	No effect	No effect	No effect	No effect
F25B5.6	*Fpgs*	*FPGS*	No effect	ND	Increased	Increased	Decreased	ND	No effect	No effect
his-12	*His2A*	*HIS2H2AB*	Increased	Increased	No effect	No effect	=	Decreased	Decreased	Decreased
sfxn-1.4	*Sfxn1-3*	*SFXN1/3*	Increased	Increased	No effect	No effect	=	Decreased	No effect	No effect
abhd-11.1	*CG2059*	*ABHD11*	Increased	=	No effect	No effect	Decreased	=	No effect	No effect
acs-1	*Acsf2*	*ACSF2*	Increased	=	No effect	No effect	Decreased	=	Decreased	No effect
crls-1	*CLS*	*CRLS1*	Increased	=	No effect	No effect	Increased	=	No effect	No effect
cyp-35A1	*Cyp18a1*	*CYP2C8*	Increased	Increased	Decreased	No effect	Decreased	=	No effect	No effect
D2023.6	*Adck1*	*ADCK1*	Increased	Increased	Decreased	No effect	=	=	Decreased	No effect
dlat-2	*muc*	*DLAT*	No effect	ND	Increased	No effect	No effect	ND	Decreased	Decreased
gpx-1	*PHGPx*	*GPX4*	No effect	ND	No effect	Increased	No effect	ND	No effect	No effect
timm-17B.1	*Tim17b*	*TIMM17A/B*	Increased	=	No effect	No effect	Increased	=	No effect	Decreased
oatr-1	*Oat*	*OAT*	No effect	ND	Increased	No effect	No effect	ND	Increased	No effect
R10H10.6	*CG2846*	*RFK*	No effect	ND	Increased	No effect	Decreased	ND	No effect	No effect
alh-12 iso B	*Aldh*	*ALDH9A1*	=	ND	Decreased	No effect	=	ND	No effect	No effect
C33A12.1	*ND-13B*	*NDUFA5*	=	ND	No effect	No effect	=	ND	No effect	No effect
K02F3.2	*aralar1*	*SLC25A12*	Increased	=	Decreased	No effect	=	=	No effect	Decreased
T10F2.2	*CG1628*	*SLC25A15*	=	ND	No effect	No effect	=	ND	No effect	No effect

bioRxiv preprint doi: https://doi.org/10.1101/2021.10.19.465059; this version posted October 20, 2021. The copyright holder for this preprint (which was not certified by peer review) is the author/funder, who has granted bioRxiv a license to display the preprint in perpetuity. It is made available under aCC-BY-NC-ND 4.0 International license.

Supplementary Information for:

Identification of novel therapeutic targets for polyglutamine toxicity disorders that target mitochondrial fragmentation

Annika Traa[1,2]*, Emily Machiela[3*], Paige D. Rudich[1,2], Sonja K. Soo[1,2], Megan M. Senchuk[3], Jeremy M. Van Raamsdonk[1,2,3,4,5]

[1]Department of Neurology and Neurosurgery, McGill University, Montreal, Quebec, H4A 3J1, Canada
[2]Metabolic Disorders and Complications Program, and Brain Repair and Integrative Neuroscience Program, Research Institute of the McGill University Health Centre, Montreal, Quebec, H4A 3J1, Canada
[3]Laboratory of Aging and Neurodegenerative Disease, Center for Neurodegenerative Science, Van Andel Research Institute, Grand Rapids MI 49503, USA
[4]Division of Experimental Medicine, Department of Medicine, McGill University, Montreal, Quebec, Canada
[5]Department of Genetics, Harvard Medical School, Boston MA 02115, USA

*these authors contributed equally to this work

bioRxiv preprint doi: https://doi.org/10.1101/2021.10.19.465059; this version posted October 20, 2021. The copyright holder for this preprint (which was not certified by peer review) is the author/funder, who has granted bioRxiv a license to display the preprint in perpetuity. It is made available under aCC-BY-NC-ND 4.0 International license.

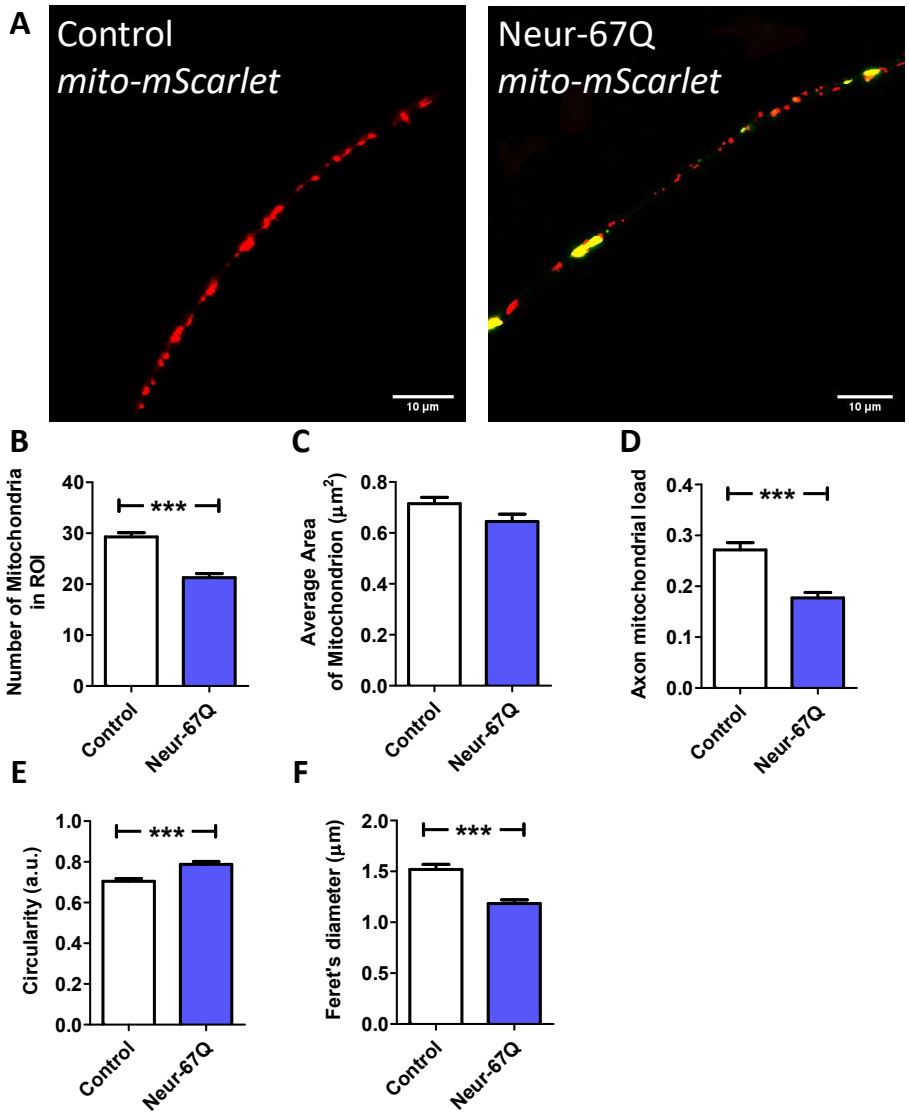

Figure S1. CAG repeat expansion disrupts mitochondrial morphology in neurons during early adulthood. Representative images of mitochondria (red) in dorsal nerve cord in control and Neur-67Q worms (**A**). Mitochondrial morphology was visualized by fusing the red fluorescent protein mScarlet to the mitochondrially-targeted protein TOMM-20 in order to target mScarlet to the mitochondria. Quantification of mitochondrial morphology reveals that Neur-67Q worms have a decreased number of mitochondria compared to control worms (**B**). While mitochondrial area is not significantly affected in Neur-67Q worms (**C**), these worms have a significant decrease in axonal mitochondrial load (**D**) compared to control worms. The mitochondria of Neur-67Q worms have increased circularity (**D**) and a decreased Feret's diameter (**E**) compared to the mitochondria of control worms. Control worms are *rab-3p::tomm-20::mScarlet.* Three biological replicates were performed. Statistical significance was assessed using a t-test (panels B-F). Error bar indicate SEM. ***p<0.001.

bioRxiv preprint doi: https://doi.org/10.1101/2021.10.19.465059; this version posted October 20, 2021. The copyright holder for this preprint (which was not certified by peer review) is the author/funder, who has granted bioRxiv a license to display the preprint in perpetuity. It is made available under aCC-BY-NC-ND 4.0 International license.

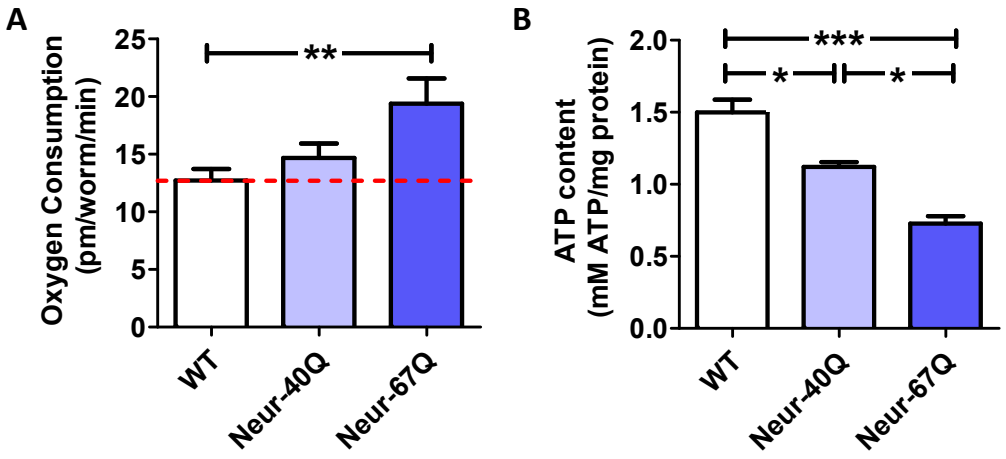

Figure S2. CAG repeat expansion in neurons disrupts mitochondrial function. Mitochondrial function in Neur-67Q worms was assessed by quantifying oxygen consumption and ATP levels. Neur-67Q worms have increased oxygen consumption (**A**) and decreased ATP levels (**B**) compared to control worms. Three biological replicates were performed. Statistical significance was assessed using a one-way ANOVA with Bonferroni's multiple comparison test. Error bar indicate SEM. *p<0.05, **p<0.01, ***p<0.001.

bioRxiv preprint doi: https://doi.org/10.1101/2021.10.19.465059; this version posted October 20, 2021. The copyright holder for this preprint (which was not certified by peer review) is the author/funder, who has granted bioRxiv a license to display the preprint in perpetuity. It is made available under aCC-BY-NC-ND 4.0 International license.

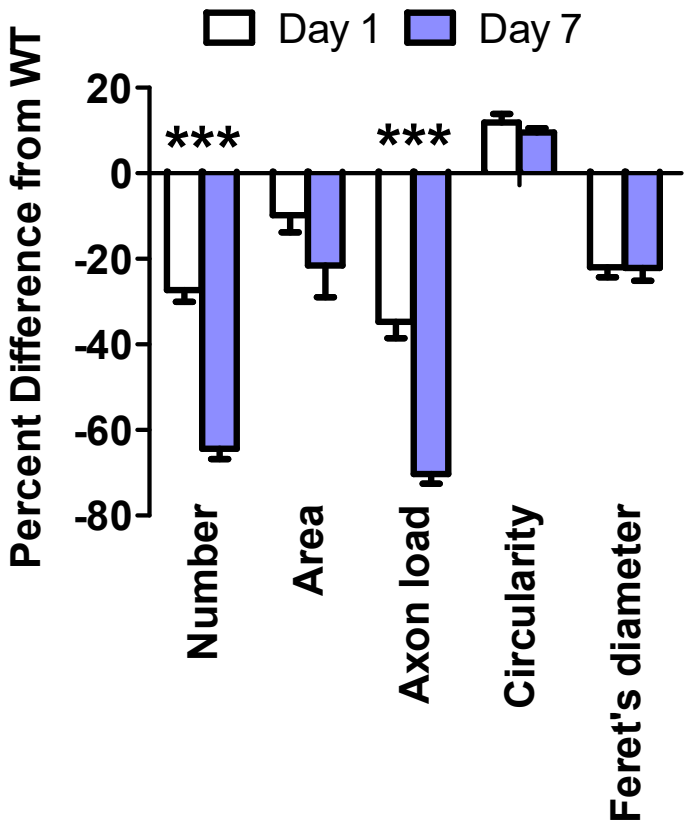

Figure S3. Differences in mitochondrial morphology in neuronal model of polyglutamine toxicity worsen with age. This figure compares the percentage change in measurements of mitochondrial morphology in Neur-67Q worms relative to wild-type worms at day 1 (**Figure S1**) and day 7 (**Figure 1**) of adulthood. The decrease in mitochondrial number and axonal mitochondrial load exhibited significantly greater deficit at day 7 of adulthood compared to day 1 of adulthood. Statistical significance was assessed using a two-way ANOVA with Bonferroni's multiple comparison test. Error bar indicate SEM. ***p<0.001.

bioRxiv preprint doi: https://doi.org/10.1101/2021.10.19.465059; this version posted October 20, 2021. The copyright holder for this preprint (which was not certified by peer review) is the author/funder, who has granted bioRxiv a license to display the preprint in perpetuity. It is made available under aCC-BY-NC-ND 4.0 International license.

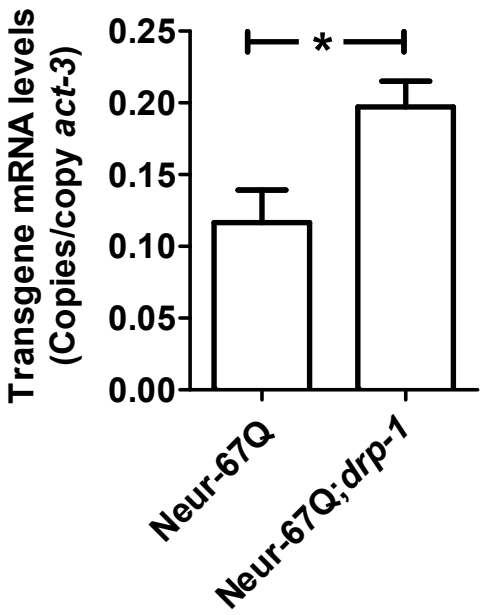

Figure S4. Deletion of *drp-1* results in increased expression of the polyglutamine transgene. mRNA was isolated from day 1 pre-fertile young adult worms. Primers were designed to target YFP. In Neur-67Q worms, deletion of *drp-1* significantly increased mRNA expression levels of the polyglutamine transgene. Bars indicate mean value of three biological replicates. Statistical significance was assessed using a t-test. Error bars indicate SEM. *p<0.05.

bioRxiv preprint doi: https://doi.org/10.1101/2021.10.19.465059; this version posted October 20, 2021. The copyright holder for this preprint (which was not certified by peer review) is the author/funder, who has granted bioRxiv a license to display the preprint in perpetuity. It is made available under aCC-BY-NC-ND 4.0 International license.

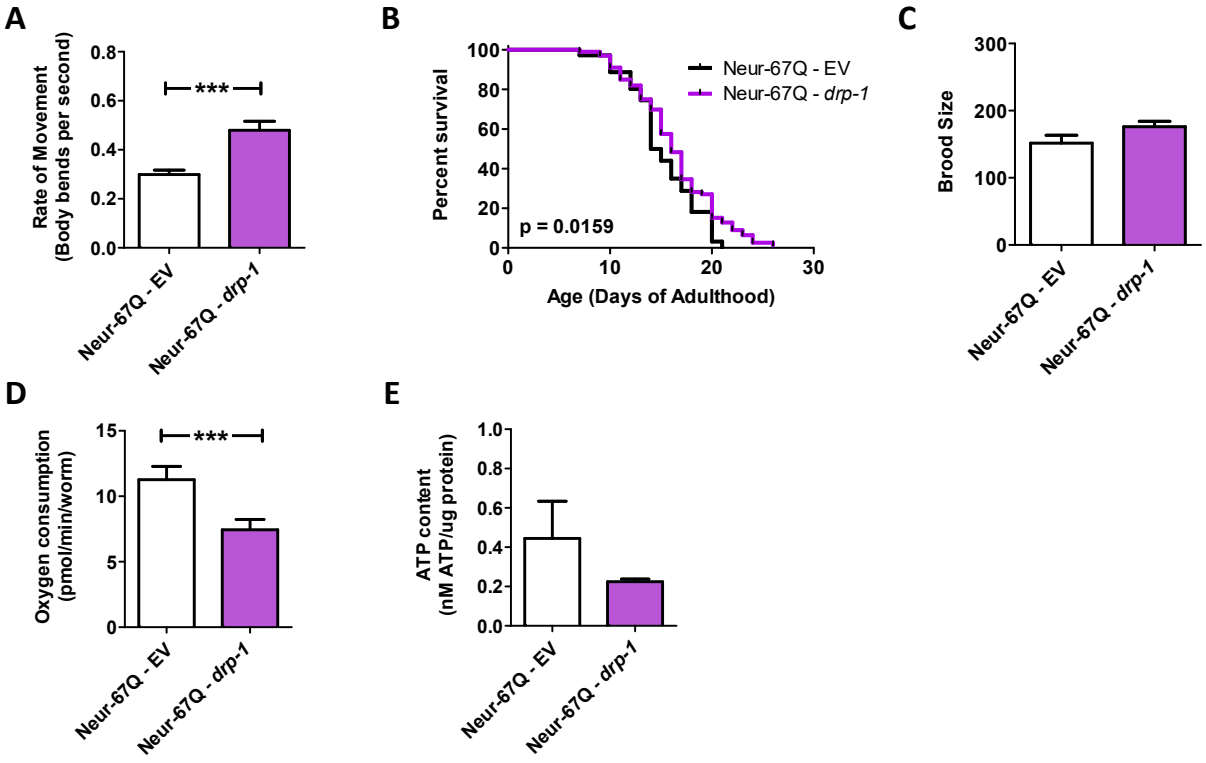

Figure S5. Decreasing mitochondrial fission through *drp-1* RNAi increases movement and lifespan in neuronal models of polyglutamine toxicity. Neur-67Q worms were crossed to *sid-1;unc-119p::sid-1* worms to allow for RNAi only in neurons. *drp-1* RNAi increases movement rates in Neur-67Q worms (**A**) and results in a small but significant increase in lifespan in Neur-67Q worms (**B**). *drp-1* RNAi has no effect on fertility in Neur-67Q worms (**C**). *drp-1* RNAi significantly reduced oxygen consumption in Neur-67Q worms (**D**) and resulted in a trend towards decreased ATP levels (**E**). A minimum of three biological replicates were performed. Bars indicate the mean value. Significance was assessed using a t-test (A,C,D,E) or log-rank test (B). Error bars indicate SEM. ***p<0.001.

bioRxiv preprint doi: https://doi.org/10.1101/2021.10.19.465059; this version posted October 20, 2021. The copyright holder for this preprint (which was not certified by peer review) is the author/funder, who has granted bioRxiv a license to display the preprint in perpetuity. It is made available under aCC-BY-NC-ND 4.0 International license.

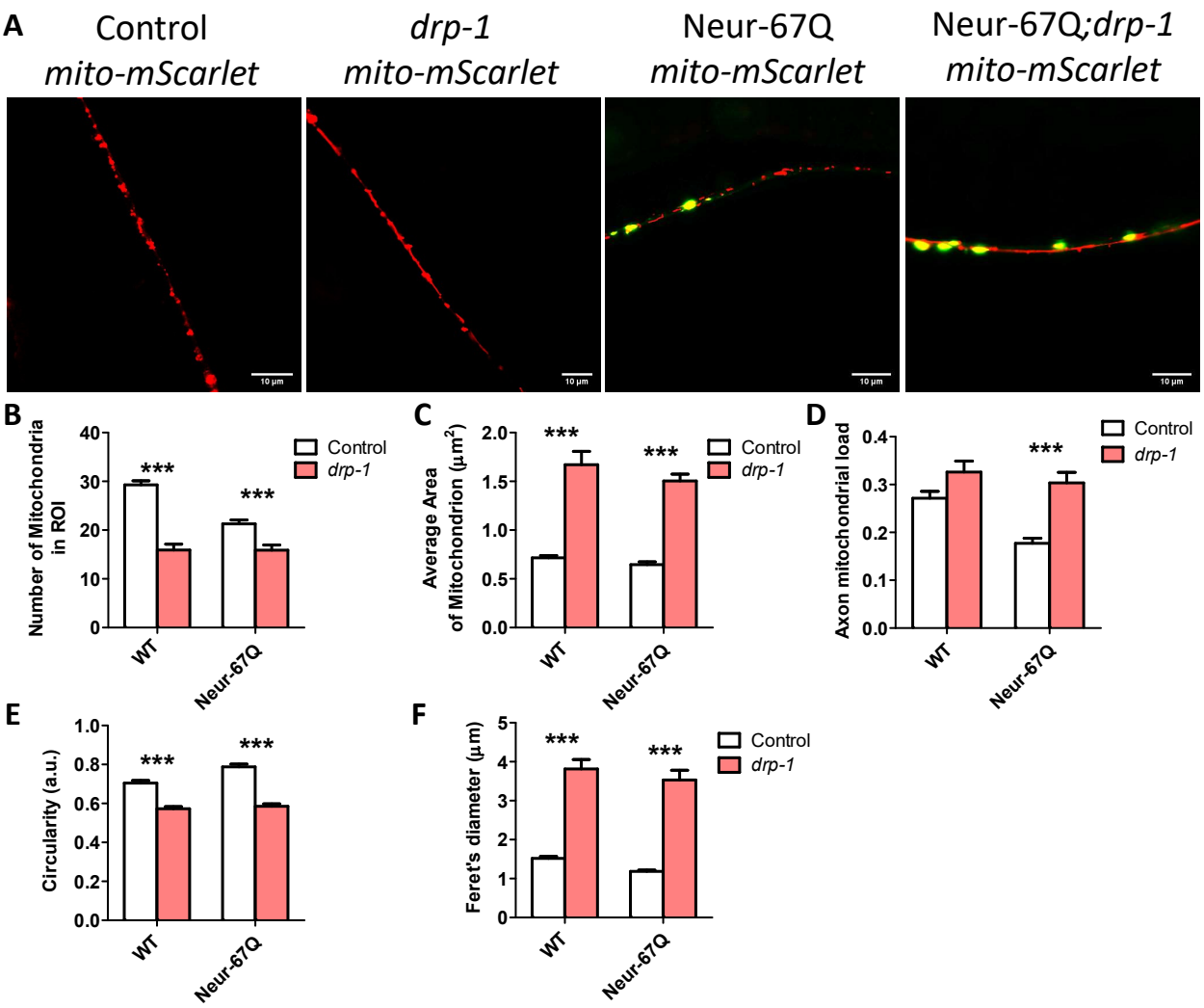

Figure S6. Disruption of *drp-1* markedly elongates mitochondria in neurons. Deletion of *drp-1* decreased mitochondrial fragmentation in Neur-67Q and control worms. Representative images of Neur-67Q worms and control worms in wild-type and *drp-1* deletion background (**A**). Quantification of mitochondrial morphology revealed that *drp-1* deletion significantly decreased mitochondrial number (**B**), increased mitochondrial area (**C**), increased axonal mitochondrial load (**D**), decreased mitochondrial circularity (**E**), and increased the Feret's diameter of the mitochondria (**F**) in both Neur-67Q and control worms. Control worms are *rab-3p::tomm-20::mScarlet.* Three biological replicates were performed. Statistical significance was assessed using a two-way ANOVA with Bonferroni posttest. Error bars indicate SEM. ***p*<0.01, ****p*<0.001.

bioRxiv preprint doi: https://doi.org/10.1101/2021.10.19.465059; this version posted October 20, 2021. The copyright holder for this preprint (which was not certified by peer review) is the author/funder, who has granted bioRxiv a license to display the preprint in perpetuity. It is made available under aCC-BY-NC-ND 4.0 International license.

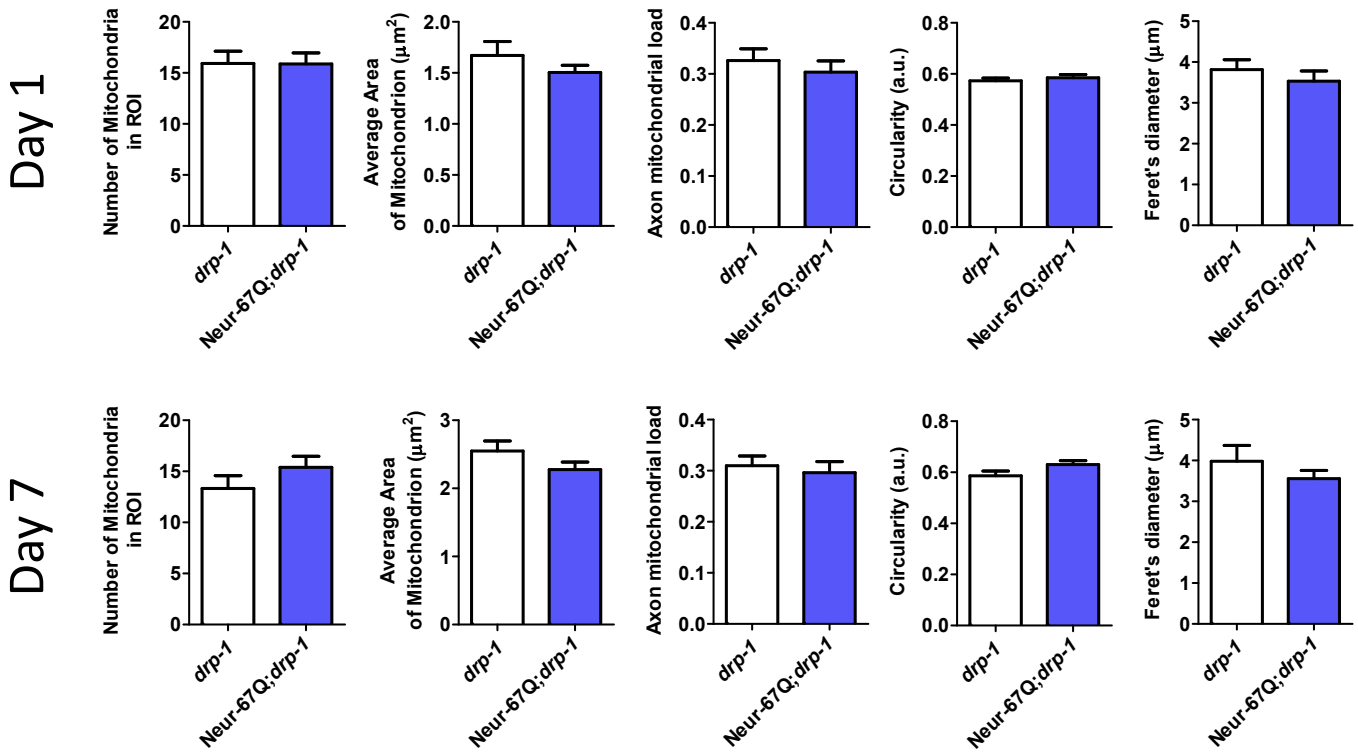

Figure S7. Expression of disease-length polyglutamine in neurons does not affect mitochondrial morphology in *drp-1* mutant background. This figure is displaying the data from **Figure 3** and **Figure S4** in such a way to directly compare *drp-1* worms to Neur-67Q;*drp-1* worms. There were no significant differences in any measure of mitochondrial morphology between *drp-1* and Neur-67Q;*drp-1* worms at day 1 (top) or day 7 (bottom) of adulthood. Thus, disruption of *drp-1* completely eliminates differences in mitochondrial morphology between Neur-67Q and wild-type worms. Three biological replicates were performed. Statistical significance was assessed using a t-test. Error bars indicate SEM.

bioRxiv preprint doi: https://doi.org/10.1101/2021.10.19.465059; this version posted October 20, 2021. The copyright holder for this preprint (which was not certified by peer review) is the author/funder, who has granted bioRxiv a license to display the preprint in perpetuity. It is made available under aCC-BY-NC-ND 4.0 International license.

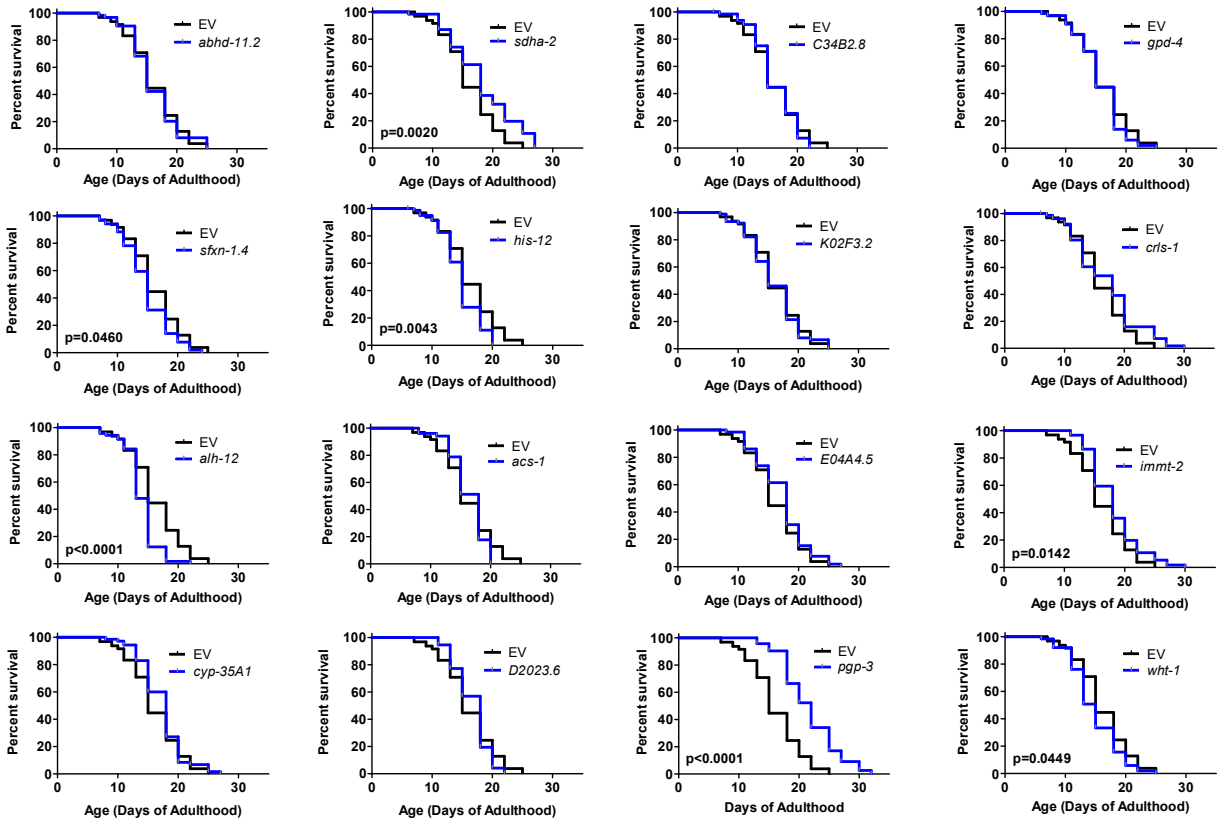

Figure S8. Neuron-specific knockdown of *sdha-2, immt-2* and *pgp-3* extends lifespan in a wild-type background. *unc-119p::sid-1;sid-1* control worms were treated with RNAi clones that decrease mitochondrial fragmentation and improved movement in Neur-67Q worms. Only three of the sixteen RNAi clones that improved movement in Neur-67Q worms resulted in increased lifespan in control worms. Three biological replicates were performed. Log-rank test was used to assess significance.

bioRxiv preprint doi: https://doi.org/10.1101/2021.10.19.465059; this version posted October 20, 2021. The copyright holder for this preprint (which was not certified by peer review) is the author/funder, who has granted bioRxiv a license to display the preprint in perpetuity. It is made available under aCC-BY-NC-ND 4.0 International license.

714 **Table S1. Comparison of neuronal and body wall muscle models of polyglutamine toxicity.**

	Wild-type	Neur-67Q model	BW-Htt74Q model
Promoter		*rgef-1*	*unc-54*
Huntingtin sequence		None	Exon 1
Glutamines		67	74
Fluorescent tag		YFP	GFP
Expression		All neurons	Body wall muscle
Mitochondrial number		Decreased	Increased
Mitochondrial area		Unchanged	Decreased
Mitochondria circularity		Increased	Increased
Oxygen consumption		Increased	Unchanged
ATP levels		Decreased	Unchanged
Movement		Decreased	Decreased
Lifespan		Decreased	Decreased
Brood size		Decreased	Decreased
Development time		Increased	Unchanged
Effect of *drp-1* deletion			
Mitochondrial morphology	Elongated	Elongated	Unchanged
Oxygen consumption	Unchanged	Decreased	Unchanged
ATP levels	Decreased	Decreased	Decreased
Movement	Unchanged	Increased	Decreased
Lifespan	Unchanged	Increased	Decreased
Brood size	Decreased	Unchanged	Decreased
Development time	Increased	Unchanged	Increased
Effect of *drp-1* RNAi			
Oxygen consumption	Unchanged	Decreased	Unchanged
ATP levels	Decreased	Decreased	Decreased
Movement	Increased	Increased	Unchanged
Lifespan	Unchanged	Increased	Increased
Brood size	Decreased	Unchanged	Decreased

715

716